Arthropod-Plant Interactions (2007) 1:221–243
DOI 10.1007/s11829-007-9021-4

ORIGINAL PAPER

Plant surface–bug interactions: *Dicyphus errans* stalking along trichomes

Dagmar Voigt · Elena Gorb · Stanislav Gorb

Received: 11 July 2007 / Accepted: 17 October 2007 / Published online: 7 November 2007

Abstract In contrast to many arthropods whose locomotion on plant surfaces is impeded by trichomes, the omnivorous mirid bug *Dicyphus errans* Wolff (Heteroptera, Miridae, Bryocorinae) lives on pubescent plants and preys on a variety of phytophagous arthropods. Morphological (slim body, long slender legs, elongated curved claws) and behavioural (locomotion) adaptations to hairy plant substrates result in higher predation effectiveness and fecundity, as well as a shorter developmental cycle of the bug compared to insects on plants without trichomes. To understand the bug–plant interactions from the biomechanical point of view, the bug's attachment system and the leaf surfaces of various plant species were analysed. Bug attachment ability was estimated in an inversion experiment on the adaxial and abaxial sides of leaves in 40 plant species. Furthermore, bug traction forces on the abaxial leaf side of 14 plant species were measured. Morphometrical variables of trichomes and the adhesive properties of plant surfaces were estimated. The bugs' traction force ranged from 0.07 mN on *Brassica oleracea* (Brassicaceae) to 1.21 mN on *Plectranthus ambiguus* (Lamiaceae) and *Solanum melongena* (Solanaceae). Bugs performed considerably better on hairy surfaces where a significant positive correlation between the force and both the trichome length and diameter was found. The trichome density and aspect ratio did not influence the force. Adhesion properties of plant surfaces covered with trichomes may also significantly impede the traction force. Based on the results obtained, it is concluded that hairy plants provide a more suitable environment for *D. errans* than either smooth ones or those covered with wax crystals. Hairy plant surfaces are predicted to support stronger attachment and therefore more reliable locomotion of the bug.

Keywords Adhesion · Attachment · Biomechanics · Bryocorinae · Heteroptera · Insect–plant interactions · Locomotion · Miridae · Traction force · Trichomes

Handling editor: Heikki Hokkanen

D. Voigt (✉) · E. Gorb · S. Gorb
Evolutionary Biomaterials Group, Department of Thin-Films and Biological Systems, Max-Planck Institute for Metals Research, Heisenbergstraße 03, 70569 Stuttgart, Germany
e-mail: voigt@mf.mpg.de

E. Gorb
e-mail: o.gorb@mf.mpg.de

S. Gorb
e-mail: s.gorb@mf.mpg.de

Introduction

Many arthropods have the ability to attach to plant surfaces. Thus, they have access to widely expanded, complex and greatly diverse habitats provided by numerous plants. More than two-thirds of the insects in Central Europe are associated with plants at least during part of their life (Zwölfer 2003). Plants play a crucial role as interactive components in the interplay between entomophagous arthropods and herbivores (Cortesero et al. 2000). Many different kinds of plant–arthropod interactions have been intensively studied, e.g. pollination and phytophagy (e.g. Bernays and Chapman 1994; Jolivet 1998; Schoonhoven et al. 2005). Numerous adaptations that evolved in both partners (insects and plants) have been reported (Southwood 1973; Becerra 2003; Grimaldi and Engel 2004).

Structural features of the plant surface have been mainly considered in the context of direct plant defense and mechanical resistance against phytophagous insects (e.g. Chapman 1977; Juniper and Jeffree 1983; Begon et al.

2006). Peeters (2002) supposed that composition of an herbivore assemblage is more strongly correlated with leaf structural traits than with chemical leaf constituents. Both epicuticular waxes and plant hairs (trichomes) are well known plant structures which act as physical barriers for phytophages causing antibiotic and antixenotic reactions in insects (Smith 2005). Plant surfaces covered with wax crystals are slippery and inaccessible substrates for many arthropod species (Stork 1980b, 1986; Jeffree 1986; Juniper 1995; Eigenbrode 1996; Brennan and Weinbaum 2001; Gorb and Gorb 2002, 2006b; Müller 2006). The impact of plant trichomes on herbivores was previously reported for representatives of several arthropod families (in particular Chrysomelidae, Aphididae, Aleurodidae, Cicadellidae, Sphingidae, Noctuidae, Tetranychidae), based mainly on the presence of trichomes (Lee et al. 1986; Haddad and Hicks 2000), their density (e.g. Fordyce and Agrawal 2001; Kowalewski and Robinson 1978; Zvereva et al. 1998; Rudgers et al. 2004), shape (Andres and Connor 2003), length (Hoxie et al. 1975; Hoffmann and McEvoy 1985; Dalin et al. 2004), and glandular function (e.g. Duffey 1986). Hook-shaped trichomes on *Phaseolus* sp. and *Passiflora* sp., for example, can impale small insects (McKinney 1938; Johnson 1953; Gilbert 1971; Pillemer and Tingey 1978; Gepp 1977). Glandular trichomes, contaminating insects with their sticky exudates, have been reported for *Solanum* spp. (e.g. Gibson 1971; Gibson and Picket 1983; Gregory et al. 1986; Lapointe and Tingey 1986; Avé et al. 1987; Malakar and Tingey 2000), *Lycopersicon* spp. (e.g. McKinney 1938; Johnson 1956; Goffreda et al. 1989; Musetti and Neal 1997; Leite et al. 1999; Ecole et al. 2001; Kennedy 2003; Simmons et al. 2003, 2004), *Nicotiana* spp. (Thurston and Webster 1962; Thurston et al. 1966; Thurston 1970; Goundoudaki et al. 2003), and *Datura* spp. (van Dam and Hare 1998; Hare and Elle 2002; Hare 2005; Hare and Smith 2005). Plant pubescence may affect population dynamics (e.g. abundance, mobility, oviposition, development, mortality), body weight, behaviour, host-plant choice and acceptance, as well as the performance and fitness of phytophagous arthropods (e.g. Ringlund and Everson 1968; Gibson 1971; Hoxie et al. 1975; Benedict et al. 1983; Roberts and Foster 1983; Zvereva et al. 1998; Malakar and Tingey 2000; Valverde et al. 2001; Ranger and Hower 2002; Andres and Connor 2003).

However, smaller and/or specialized (mostly long-legged) species having an ability to attach and live on waxy and hairy plant surfaces, sometimes benefit from predator/parasitoid-free space, because natural enemies and their influence on regulation of phytophagous arthropods may be negatively affected by plant phenotypic characteristics (Kennedy 1986; Kareiva and Sahakian 1990; Coll 1998; Gassman and Hare 2005).

Such predators as representatives of Coccinellidae, Chrysopidae, and Anthocoridae may be hampered in their mobility on thick wax blooms (Shah 1982; Grevstad and Klepetka 1992; Eigenbrode 1996, 2004; Eigenbrode et al. 1996). For pubescent surfaces, Shanower et al. (1996) found that the longer and denser the trichomes are, the less are the number of pest insects that occur. Moreover, searching and consumption times become longer, and natural enemies are more frequently chemically repelled. The walking speed, searching efficiency, and encounter rate of Coccinellid larvae have been reported to be reduced on hairy plant substrates (Shah 1980, 1982; Belcher and Thurston 1982; Obrycki and Tauber 1984; Carter et al. 1984; Grevstad and Klepetka 1992). The ladybird beetles themselves and their integument may also be harmed particularly by hook-shaped trichomes (Putman 1955; Walters 1974; Dixon 1986; Quilici and Iperti 1986; Obrycki 1986; Eisner et al. 1998). Some species of Chrysopidae are hindered by a highly dense pubescence (Arzet 1972; Elsey 1974; Dos Santos et al. 2003; Simmons and Gurr 2004, 2005). Predacious thrips have been observed to be impaled by hooked trichomes (Sengonca and Gerlach 1984). Parasitoids are frequently deterred and hurt by the complex pubescence of plant surfaces (Rabb and Bradley 1968; Keller 1987; Andow and Prokrym 1990; Kashyap et al. 1991; Jervis and Kidd 1996; Gingras and Boivin 2002). True bug larvae of the family Anthocoridae have been reported to be entangled by hooked and glandular trichomes (Evans 1976; Coll et al. 1997).

Although contact phenomena and mechanical interactions between insect tarsi and plant surfaces are very important in insect–plant interactions, they have been relatively rarely studied in detail. The effect of different characteristics of the plant surface on attachment and locomotion of insects has been reported formerly in Chrysomelidae: *Phaedon chochleariae* Fab. (Stork 1980b), *Chrysolina fastuosa* Scop. (Gorb and Gorb 2002, 2006b), *Gastrophysa viridula* de Geer (Gorb and Gorb 2006a), Coccinellidae: *Adalia bipunctata* L. (Gorb et al. 2005), Calliphoridae: *Calliphora vicina* R.-D. (Gaume et al. 2004; Gorb et al. 2004), Aphididae: *Megoura viciae* Buckt. (Lees and Hardie 1988), several Formicidae (Federle et al. 1997, 2000), and Pyrrhocoridae: *Pyrrhocoris apterus* L. (Gorb et al. 2004). However, pubescent plant surfaces were considered only by Gorb and Gorb (2002) for *C. fastuosa* attachment ability on various plant surfaces, and by Betz (2002), estimating climbing performance of several *Stenus* spp. (Staphylinidae) on the adaxial side of leaves in *Glyceria maxima* (C. Hartm.) Holmb. and *Phragmites communis* Trin. (Poaceae).

Some predatory insect species, such as the palaearctic mirid bug *Dicyphus errans* Wolff (Heteroptera, Miridae, Bryocorinae), prefer hairy plant surfaces as a substrate for living, and for prey capture. Our previous bionomical

studies have demonstrated a higher fecundity and predation efficiency, as well as a shorter developmental cycle of the bug on hairy plant surfaces compared to smooth ones (Voigt 2004, 2005). This generalized mirid bug lives omnivorously on various host plants and preys on a wide range of small arthropods. Plants play a crucial role for this bug species as protected habitat, hunting ground, oviposition site as well as a source of water and nutrition. Similar to other representatives of the tribus Dicyphini among the subfamily Brycorinae (Miridae, Heteroptera), *D. errans* seems to be adapted to live on and to adhere to hairy and glandular hairy plant surfaces because of morphological and behavioural adjustments. The dicyphine bugs stalk rather quickly along plant trichomes, using their long and slender legs (Kullenberg 1946; Wheeler 2001; Voigt 2005). Using video-recordings, Southwood (1986) described several modi of locomotion of *D. errans* on a glandular hairy *Ononis* sp. surface. The bug's body is held away from the plant surface, whereas the long tibiae are oriented almost vertically and the claw is at an angle parallel to the plant surface. The hind tibiae are especially long, so that the hind femur is situated above body height. Moving one leg, the femur is raised and the tibia moved almost vertically, without contacting any trichome. The mirid bugs have a small contact area with the plant surface and adhere to trichomes only with tarsal tips, the claws, mostly without encountering the lamina between trichomes. One part of the paired claw, supported by adhesive organs (pseudopulvilli and parempodia), may grip precisely one single trichome. These claws are called "*Dicyphus*-like" with large "pseudoarolia" (pseudopulvilli) (Seidenstücker 1967) and narrow "shepherd's crook" (Southwood 1986), and are thought to enable the bug's attachment to trichomes. Wigglesworth (1959) and Jordan (1962) have assumed that adhesive organs enable the dicyphine bugs to attach not only to plants, but to smooth surfaces as well. Although the function of pulvilli and pseudopulvilli in trichome-stalking Heteroptera is not really understood, Wagner (1955) has supposed that true bugs with long, free pseudopulvilli are adapted to live on plant surfaces covered with sticky trichomes.

The goal of this study was to analyse the influence of different plant surfaces, in particular pubescent ones, on the attachment of the predatory mirid bug *D. errans* and the role of biomechanics in the bug–plant relationship.

Three main questions were asked: (1) Does the generalist *D. errans* demonstrate equal attachment ability on different plant surfaces? (2) How do different types of plant surfaces affect the locomotion and attachment force of *D. errans*? (3) Which insect–plant interactions, related to the attachment ability, can be quantitatively analysed, considering the bug tarsal morphology, trichome geometry, and plant surface adhesive properties?

The pretarsal morphology of *D. errans* was microscopically analysed. The adaxial and abaxial leaf surfaces of 40 plant species belonging to 25 families were screened according to the mirid bug attachment strength in an inversion experiment. Furthermore, 14 of these species were used in traction force tests. Leaf surfaces were described and classified into several types. Adhesive properties, trichome length and diameter of the different leaf surfaces used in the traction force test were measured and the density of hairs estimated.

Materials and methods

Insects

Adults of *Dicyphus errans* were taken from a stock culture, reared on the host plant *Plectranthus ambiguus* Bolus and Codd (Lamiaceae) with several arthropod prey species at a temperature of 22 ± 5°C/20 ± 3°C day/night, a relative humidity between 60 and 70%, and a 16 h photoperiod.

Detailed information about the attachment system was obtained from light, fluorescence, and scanning electron microscopy. Fresh tarsi of adult bugs were cut off with a razor blade, mounted on glass slides in polyvenylalcohol (Moviol), covered with glass cover-slips, and observed in a fluorescent microscope Zeiss Axioplan, equipped with HBO 103 mercury vapor lamp and XBO 75 xenon short-arc lamp (Carl Zeiss MicroImaging GmbH, Jena, Germany) as well as an integrated digital video-camera AxioCam MRc (AxioVision GmbH, München-Hallbergmoos, Germany). Fluorescence microscopy was used to localize the elastic protein resilin in the pretarsus. This protein has an auto-fluorescence with an emission maximum at 420 nm (Andersen and Weis-Fogh 1964). Superimposed digital images, obtained at green (excitation 512–546 nm, emission 600–640 nm), red (excitation 710–775 nm, emission 810–890 nm), and UV wavelengths (excitation 340–380 nm, emission 425 nm) were analysed to assess the presence of resilin (Gorb 1999).

Scanning electron microscopy studies were carried out using a cryo-SEM Hitachi S-4800 (Hitachi High-Technologies Corp., Tokyo, Japan) equipped with a Gatan ALTO 2500 cryo-preparation system (Gatan Inc., Abingdon, UK). Fresh samples of mirid bug legs were mounted on metal holders, frozen in the preparation chamber at −140°C, sputter-coated with gold–palladium (3 nm) and examined in a frozen state in the cryo-SEM at 3 kV and −120°C. From digital images of 10 randomly selected pretarsi of adult specimens, the inner length of the claw, diameter of a circle fitting the concavity of the claw, and length of the setiform parempodia were estimated, using Sigma Scan Pro 5 (SPSS Inc.) software. To observe, in

detail, how the claw interlocks with a single plant trichome, live insects attached to pubescent plant surfaces were prepared, following the same cryo-SEM procedure as described above.

Plant surfaces

The screening of plant surfaces in the inversion experiment included 40 plant species and cultivars with different surface types, belonging to 25 plant families (30 herbs, 6 lianas, 2 shrubs, 1 tree). Single leaves, located between the top and the middle of the plants, were collected at the Botanical Garden of Dresden University of Technology (Dresden, Germany). To define the type of plant surface, fresh leaves were studied using a binocular microscope Leica MZ 12.5 with integrated digital video-camera Leica ICA (Leica GmbH, Wetzlar, Germany). For detailed surface description, fresh plant samples were cut off with a razor blade, mounted on metal holders, and examined in cryo-SEM as described above for insects.

The abaxial leaf surfaces of 14 plant species (10 families), belonging to different surface types, were tested in the traction force experiment with females of *D. errans*. In hairy surfaces, the trichome length, density per 1 mm^2, and diameter (in the middle part of the trichome) were estimated from digital images and SEM-micrographs using Sigma Scan Pro 5 (SPSS Inc.) software. The values were averaged for all trichome types occurring on one leaf surface, except for peltate and clavate ones, which obviously did not allow the bug to attach according to preliminary observations. The aspect ratio of trichomes was calculated using the estimated mean values of the trichome length and diameter. To assess the trichome density, only the visible trichome bases in randomly selected areas were considered.

Adhesion force measurements of plant surfaces

For 14 abaxial leaf surfaces used in traction force experiment, adhesive properties were estimated in the adhesion force test. The measurements were carried out using a force transducer (10 g capacity, Biopac Systems Ltd., Santa Barbara, CA, USA), attached to a motorised micromanipulator DC3314R with controller MS314 (World Precision Instruments Inc., Sarasota, FL, USA). Fresh plant samples (2 cm^2) were cut out with a razor blade and mounted, with the abaxial side up, on a horizontal plexiglass stage using double-sided tape (Fig. 1). A polished sapphire ball (500 μm diameter corresponding to the total claw length as supposed contact area between mirid bug tarsi and plant surface if all claws are interlocked with trichomes, Good Fellow Cambridge Limited, Huntingdon, UK) was glued to an insect pin (diameter 0.25 mm, original Karlsbader, Germany) with superglue (ergo 5300, Kisling Deutschland GmbH, Schwäbisch Hall, Germany). The sapphire ball was used because it is regularly shaped, smooth, and chemically neutral which gives the possibility to compare adhesive properties of different surfaces. The pin was firmly attached to the force transducer. The sapphire ball was moved continuously with a velocity 20 μm/s, brought in contact with the leaf surface, pre-loaded to maximum 20 μN force, and then withdrawn while the pull-off force was measured. Force-time curves were used to estimate the maximum pull-of (adhesion) force. For each plant surface, 20 measurements on different sites, and 280 single measurements in total were carried out (N = 14 plant species, n = 20 measurements per plant species). Kruskal–Wallis one way ANOVA on ranks followed by all pairwise multiple comparision procedures (Tukey test) was used to evaluate differences in the adhesion force values between plant surfaces (software SigmaStat 3.1.1®, Systat Software, Inc., Richmond, California, USA). The relationship between traction force values and plant surface adhesion was analysed by linear regression method.

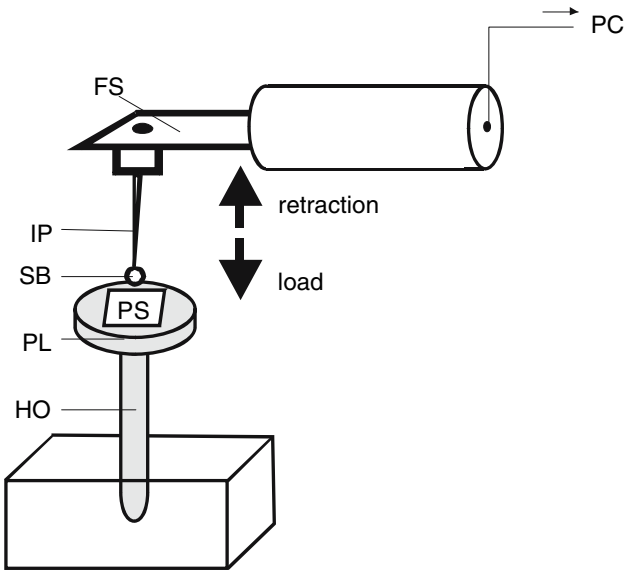

Fig. 1 Experimental setup for estimation of adhesive properties in plant surfaces. The freshly cut plant sample (PS) was attached to a horizontal platform (PL) on a holder (HO). A sapphire ball (SB) was glued to an insect pin (IP), adhered to a force sensor (FS). The sensor with ball was moved with a motorized micromanipulator until contact between the sapphire ball and plant surface was formed at a load of 0.2 mN, and then pulled back. The sensor signal was recorded and processed further in the computer (PC)

Inversion experiment

A bug specimen was placed on the plant surface (adaxial or abaxial leaf side), and the surface then inverted (180°). As

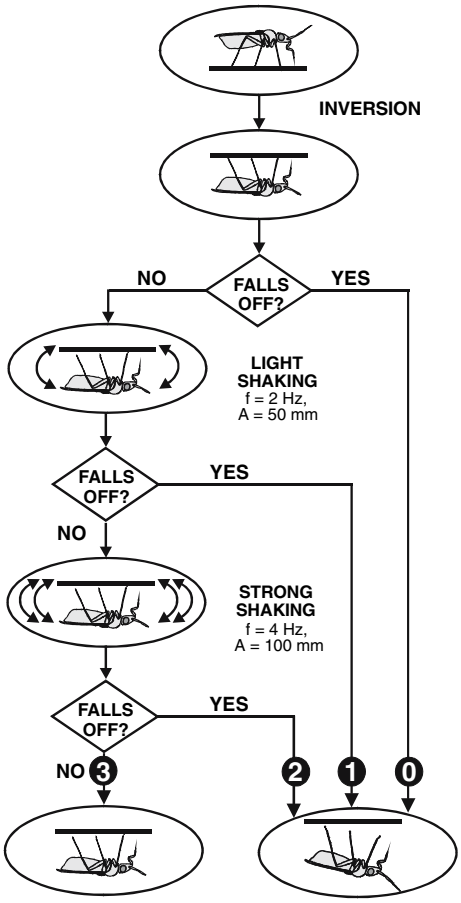

Fig. 2 Scheme of the inversion experiment, carried out on both abaxial and adaxial leaf surfaces of 40 plant species to estimate the attachment ability of *Dicyphus errans*. Four categories of the attachment strength were assigned: (0) fell immediately after inversion, (1) fell after inversion and light shaking (f = 2 Hz, A = 50 mm), (2) fell after inversion and strong shaking (f = 4 Hz, A = 100 mm), and (3) did not fall at all

shown in Fig. 2, the attachment ability was categorised as follows: the specimen (0) fell immediately after inversion, (1) fell after inversion and slight shaking at a frequency (f) of 2 Hz and an amplitude (A, up and down shaking movements) of 50 mm, (2) fell after inversion and strong shaking (f = 4 Hz, A = 100 mm), and (3) did not fall at all. Shaking was conducted considering the plant movement by wind and other environmental influences to which the bugs may be exposed in nature. In order to allow the specimen to rest between different plant surface trials, the bugs were allowed to walk over dry filter paper for 3 minutes. For each leaf surface, 5 females and 5 males were tested. The sequence of plant species used in the experiment was varied randomly. A total of 800 individual inversions (N = 80, n = 10 adult bugs) were carried out at 23 ± 2°C and 55 ± 3% relative humidity. Data were analysed by χ^2 analysis of contingency tables (software SigmaStat 3.1.1®, Systat Software Inc., Richmond, California, USA).

Traction force experiment

Traction force measurements were carried out according to Gorb et al. (2004) using a force transducer (as described above for adhesion experiments). Insects were anaesthetised with CO_2 and attached to a 10 cm long human hair with a small molten wax droplet and their forewings glued together. Bugs were weighed using an analytical balance AG 204 Delta Range (Mettler Toledo GmbH, Greifensee, Switzerland). Following anaesthesia, insects were allowed to recover for one hour, after which the free end of the hair was connected to the force sensor. Fresh plant samples with an area of 5–25 cm^2 were cut out with a razor blade from the middle part of leaves (6-leaf-stage plants) and attached to a horizontal glass plate using double-sided tape. The traction force was measured in *D. errans* females, walking distally on the abaxial leaf surface and on a glass surface, used as a reference substrate before and after walking on the plant surface. Force–time curves were used to estimate the maximal traction force produced by bugs within 30 s of the experiment on the different test substrates. For each plant surface, five individual females were tested. Totally, 70 individual tests with 70 different specimens were carried out (N = 14 plant species, n = 5 individual tests). One way ANOVA followed by all pair-wise multiple comparision procedures (Tukey test) was applied to find out differences in force between plant surfaces (software SigmaStat 3.1.1®, Systat Software, Inc., Richmond, California, USA). The relationship between absolute force values and pubescent plant surface parameters was analysed using a linear regression method. Paired *t*-test was used to calculate differences in the traction force on glass before and after plant surface trials. A posteriori, traction force measurements on glass allowed an estimation of possible tarsus contamination during walking on plant surfaces. To visualize contamination of the bug's attachment system, feet of randomly selected specimens were cut off with a razor blade immediately after testing on the plant, without allowing the specimen to groom. These were mounted on holders by means of conductive carbon double-sided adhesive tape, air-dried, sputter-coated with gold-palladium (10 nm) and observed in the SEM at 3 kV and room temperature. The degree of tarsus contamination was estimated from SEM-micrographs as proportion of contaminated area to the entire pretarsus area, averaged for 5 randomly selected pretarsi for each tested plant surface.

Results

The attachment system of *Dicyphus errans*

The inner length of the claw (n = 10), without considering the basal lobe-like structure, was 74.0 ± 10.9 μm (claw

tooth length: 2.5 ± 0.7 µm). The parempodia were 38.7 ± 5.6 µm long. The average diameter of an ideal circle fitting the concavity of the claw was 16.6 ± 0.9 µm.

The fluorescence microscopy images (Fig. 3A, B) showed the presence of resilin, an elastic protein, in the material of pseudopulvilli and membraneous areas surrounding the unguitractor plate, especially in their transitional region to the claw base. As shown in the cryo-SEM micrographs (Fig. 3C–E), the pretarsus of *D. errans* consists of an unguitractor plate bearing paired, narrow, elongated claws (ungues) with a basal lobe-like structure and a tapered tooth at the tip, two approximately equilateral trapezium-shaped rounded pseudopulvilli as well as two thin setiform parempodia. Dorsally, a stronger seta arises from the third tarsomer. The claws are strongly curved close to their basal lobe-like thickening and slightly curved only distally, while the shaft is almost straight. The claw surface has longitudinal groove-like striae, and is somewhat chiseled, polygonal in the cross section. The ventral side of the pseudopulvilli is smooth (Fig. 3D), whereas the dorsal side is structured with nearly parallel-oriented grooves, 0.5 µm apart, ending at about 1 µm to the distal margin of the pseudopulvilli (Fig. 3C).

According to ocular and cryo-SEM observations of bug locomotion on *Nicotiana sylvestris* (Fig. 3F), a single claw of the pair present on the tarsus, interlocks with a single trichome, using the border between the basal lobe-like structure and the ventral surface of the claw shaft that apparently leaves an imprint in the trichome wall (Fig. 3F, arrowhead). The use of the pseudopulvilli and parempodia in claw interlocking with trichomes was not observed.

Plant surface characterisation

A great variety of plant surfaces studied requires systematic description (Appendix) and classification following the parameters defined in Fig. 4. A plant surface may be generally smooth, waxy or hairy, however, combinations of these features frequently occur. Various structures can even be found on the same plant organ (Fig. 4A). We distinguished six types of plant surfaces in this study (Fig. 8): (1) smooth (*s*), (2) waxy (*w*), (3) mixed waxy and hairy (*wh*), (4) hairy (*h*), (5) glandular hairy (*g*), as well as (6) mixed hairy and glandular hairy (*hg*). *Smooth* plant surfaces (*s*) lack both wax crystals and trichomes. Their surface topography is determined only by cell irregularities and leaf veins. *Waxy* plant surfaces (*w*) bear epicuticular crystalline waxes, defined in our description according to the terminology of Barthlott et al. (1998). Some surfaces

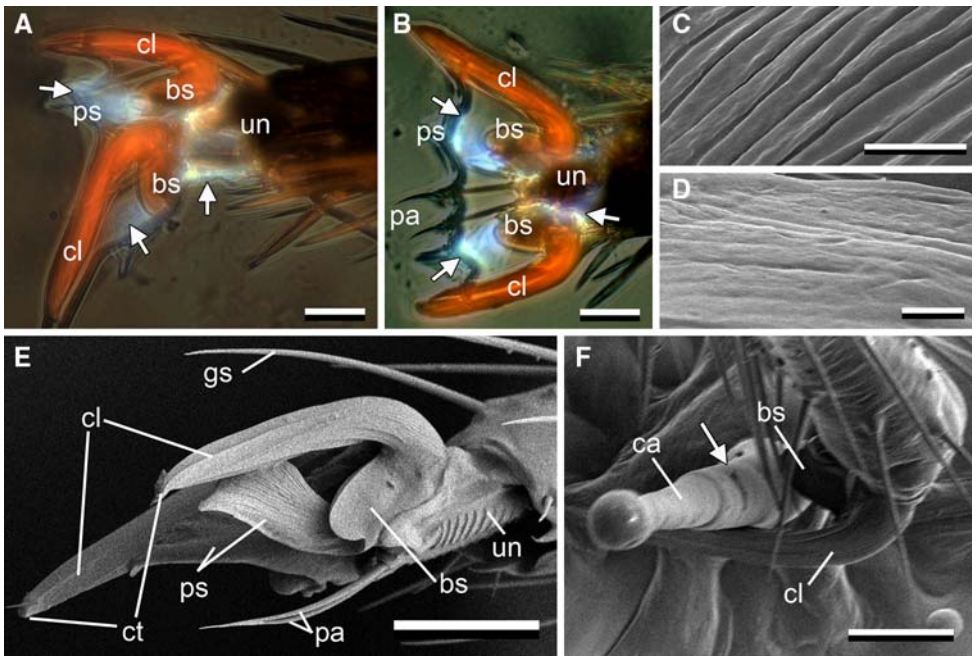

Fig. 3 Attachment system of *Dicyphus errans*. The pretarsus bears an unguitractor plate (*un*), paired curved claws (*cl*) each with a claw tooth (*ct*), and basal lobe-like structure (*bs*), pseudopulvilli (*ps*), setiform parempodia (*pa*), stronger, so called guard setae (*gs*). (**A**, **B**) Shiny blue areas in fluorescence light microscopy images demonstrate the presence of resilin in the pseudopulvilli and the membranous areas surrounding unguitractor plate (arrows); dorso-lateral view (**A**), dorsal view (**B**). (**C**, **D**) Cryo-SEM micrographs showing the surface structure of the dorsal (**C**) and ventral sides (**D**) of the pseudopulvillus. (**E**) The whole pretarsus. (**F**) The claw interlocking with a glandular capitate trichome (*ca*) of *Nicotiana sylvestris;* arrow points to a transverse imprint of the trichome stem, possibly caused by bug claw attachment. Scale bars: **A**, **B**, **E**, **F** = 25 µm; **C**, **D** = 2 µm

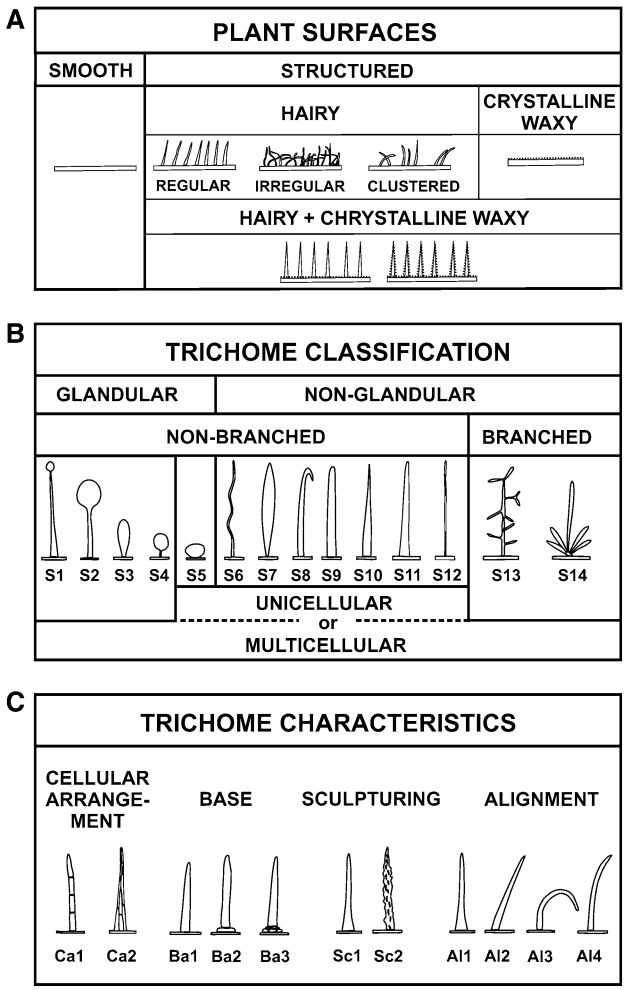

Fig. 4 (**A**, **B**) Diagrams of plant surfaces and trichome types found on the tested leaves. The diagrams are based on the trichome arrangement, cellular arrangement in the single trichome, its function, and shape: (*S1*) cone-shaped with glandular head; (*S2*) capitate; (*S3*) clavate, club-shaped; (*S4*) stalked glandular heads; (*S5*) peltate; (*S6*) spiral-shaped; (*S7*) spindle-shaped; (*S8*) hook-shaped; (*S9*) finger-shaped; (*S10*) dart-shaped; (*S11*) cone-shaped; (*S12*) thread-shaped; (*S13*) tree-shaped, dendroid; (*S14*) star-shaped, stellate. (**C**) Diagram showing the characteristics of trichomes found on the tested leaf surfaces. The diagram is based on the trichome alignment, surface texture, base structure and cellular arrangement. (*Al1*) perpendicular; (*Al2*) inclined; (*Al3*) curved; (*Al4*) bent; (*Sc1*) smooth; (*Sc2*) nodose; (*Ba1*) without base/socket; (*Ba2*) unicellular socket; (*Ba3*) multicellular socket; (*Ca1*) uniseriate; (*Ca2*) multiseriate

have both types of surface structures: *hairs and wax* crystals (*wh*). *Hairy* surfaces (*h*) are defined as those, covered with non-glandular trichomes, whereas *glandular hairy* surfaces (*g*) bear glandular trichomes. Some surfaces bear both these trichome types (*hg*). Most of the species studied belong to the mixed non-glandular hairy and glandular hairy type (*hg*). 13 species have this surface type on both sides of the leaf; 17 or 16 species have it on either the adaxial or abaxial surface, respectively. Eleven species were covered with epicuticular wax crystals (*w*) on the adaxial and 6 species—on the abaxial leaf surface. Several species bear waxes on both sides of the leaf (*B. oleracea*, *B. semperflorens*, *C. persicum*, *S. hoffmanii*, *L. sativa*, and *V. tricolor*). Three species' adaxial leaf sides and five species' abaxial surfaces were covered with both crystalline waxes and trichomes (*wh*). The hairy plant surface type (*h*) as well as the glandular hairy one (*hg*) are each represented in 4 species adaxially and 6 species abaxially. Only *S. media* has no outgrowths on either side of the leaf (*s*). At the family level, no characteristic surface type is distinguished. For example, representatives of Asteraceae examined bear epicuticular crystalline waxes (*L. sativa*), a combination of epicuticular crystalline waxes and either non-glandular (*G. jamesonii*) or glandular trichomes (*C. officinale*).

Although many attempts have been undertaken by previous authors to classify a great variety of trichomes (e.g. Hummel and Staesche 1962; Uphof 1962; Esau 1965; Napp and Zinn 1973; Johnson 1975; Payne 1978; Metcalfe and Chalk 1988), there is no generally accepted terminology. To describe the trichomes found on the plants used in our study, their indumentum, cellular arrangement, function, branching, shape, surface sculpturing, base, and orientation were considered (Fig. 4).

Trichomes occur regularly or irregularly, sparsely, dispersed, numerously or densely. They may be uni- or multicellular. The latter may consist of either one (uniseriate, Fig. 4C, *Ca1*) or two and more rows of cells (multiseriate, Fig. 4C, *Ca2*). We also distinguished non-glandular and glandular trichomes. Glandular trichomes contain secretions, often accumulated in rounded heads. Capitate glandular trichomes (Fig. 4B, *S1* and *S2*) bear conspicuous uni- or multicellular stalks having glandular heads on their tips (diameter of the head is smaller than the stalk length). Peltate glandular trichomes (Fig. 4B, *S5*) are uni- or multicellular globular glandular heads. Stalked glandular heads (Fig. 4B, *S4*) have very short stalks, the length of which is smaller than the diameter of their heads. Clavate glandular trichomes (Fig. 4B, *S3*) are club-shaped and mainly multicellular. Non-glandular trichomes can be distinguished according to their various shapes. Besides the cone-shaped ones (Fig. 4B, *S11*), frequently occurring in plant surfaces studied, trichomes may have shapes similar to spirals (Fig. 4B, *S6*), threads (Fig. 4B, *S12*), hooks (Fig. 4B, *S8*), fingers (Fig. 4B, *S9*), darts (Fig. 4B, *S10*) or spindles (Fig. 4B, *S7*). Trichomes are usually aligned in one preferred direction. Some of them form a right angle with the leaf surface (perpendicular orientation) (Fig. 4C, *Al1*). Inclined trichomes are sloped (Fig. 4C, *Al2*), bent trichomes are slightly arcuated (Fig. 4C, *Al4*), whereas curved ones have a stronger deflection, up to 180° and more (Fig. 4C, *Al3*). The trichome surface may be smooth (Fig. 4C, *Sc1*) or rough at the microscale level with nodose knobby irregular outgrowths (protuberances) (Fig. 4C,

Sc2). Trichomes may emerge only from the leaf epidermis (Fig. 4C, *Ba1*), or be based on a mostly convex uni- (Fig. 4C, *Ba2*) or multicellular socket (Fig. 4C, *Ba3*). A detailed description of studied plant surfaces is given in the Appendix and Figs. 5–7.

The quantitative analyses of trichomes on 14 abaxial leaf surfaces used in traction force tests, showed that trichomes differ strongly in their shape, anatomy, orientation, length, diameter, density, and aspect ratio (Table 1). Even on one single surface, trichomes may be very heterogeneous. The averaged trichome length ranged from 262.1 µm in *C. annuum* to 650.4 µm in *P. ambiguus*. The thinnest trichomes were found in *F.* × hybrida (15.4 µm), and the thickest ones in *C. hirsuticaulis* (87.7 µm). On *F.* × hybrida, the lowest density of trichomes was recorded (2.6 mm^{-2}), and in the domatia of *C. annuum* the highest (70.6 mm^{-2}). The trichomes of *C. annuum* and *C. hirsuticaulis* had the lowest aspect ratio (6.1 and 7.3, respectively), whereas those of *F.* × hybrida and *Gerbera jamesonii* × hybrida had the highest (22.6 and 16.1, respectively).

The values of measured adhesion force varied in different plant species (Table 1). The highest force was recorded in *N. sylvestris* (median: 207.0 µN), and the lowest one in *G. jamesonii* (median: 4.5 µN) (Kruskal–Wallis one way ANOVA on ranks, Tukey Test, $H_{13,279} = 143.989$, $P \leq 0.001$). Referring to plant surface types, the adhesion force on hairy surfaces (*h*, median: 55.2 µN), glandular ones (*g*, median: 43.5 µN), as well as non-glandular and glandular hairy ones (*hg*, median: 33.2 µN) were significantly higher than on surfaces covered with wax crystals (*w*, median: 5.1 µN) and both wax crystals and trichomes (*wh*, median: 4.5 µN) (Kruskal–Wallis one way ANOVA on ranks, $H_{5,279} = 82.399$, $P \leq 0.001$). Further significant differences were found between *h* and *hg* surfaces.

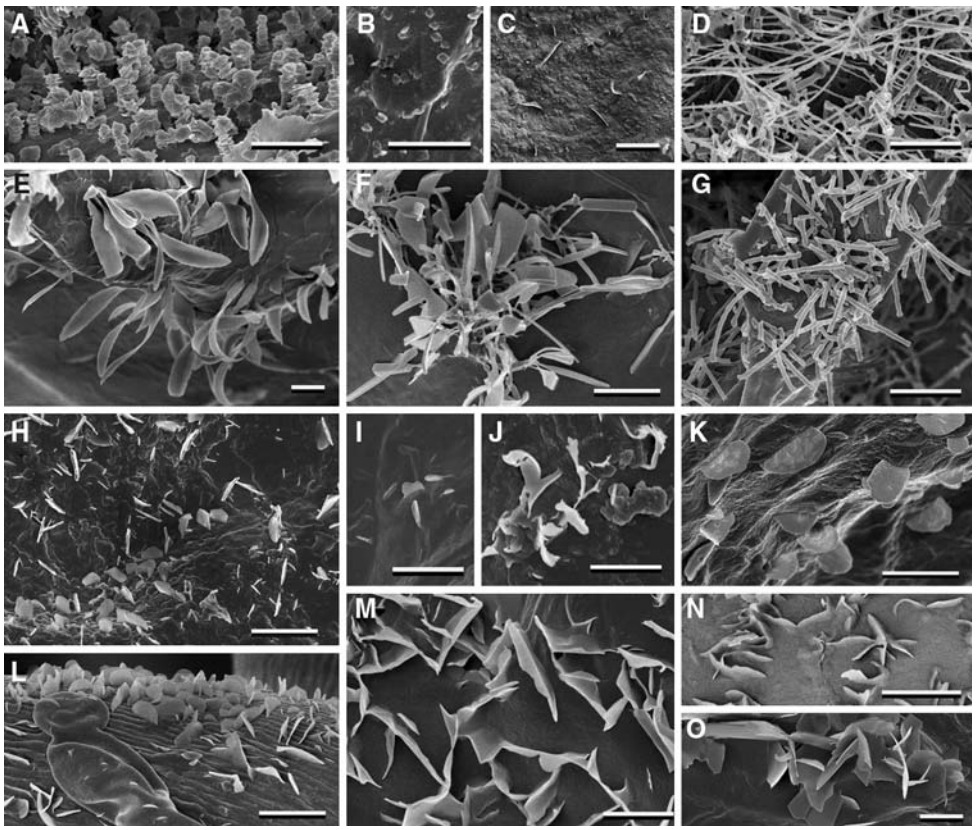

Fig. 5 Cryo-SEM micrographs of plant surfaces covered with epicuticular crystalline waxes used in the experiments with *Dicyphus errans*. (**A**) *Aristolochia elegans*, abaxial surface covered with transversely ridged rodlets. (**B**) *Begonia semperflorens*, abaxial surface, polygonal granules. (**C**) *Begonia semperflorens*, adaxial surface, membraneous entire platelets. (**D**) *Brassica oleracea*, adaxial surface, filamentous crystals. (**E**) *Lactuca sativa*, adaxial surface, rosettes of membraneous platelets. (**F**) *Hibiscus rosa-chinensis*, adaxial side, clusters of platelets. (**G**) *Tropaeolum majus*, abaxial side, tubules. (**H**) *Fuchsia* × hybrida, adaxial side, platelets. (**I**) *Capsicum annuum*, adaxial side, group of platelets. (**J**) *Rosa* × hybrida, adaxial side, platelets. (**K**) *Cyclamen persicum*, abaxial side, plates. (**L**) *Malus domestica*, abaxial side, cluster of platelets on the trichome. (**M**) *Malus domestica*, abaxial side, irregular membraneous platelets. (**N**) *Syngonium auritum*, abaxial surface irregular membraneous platelets. (**O**) *Viola tricolor*, adaxial side, grouped polygonal plates surrounding stomata. Scale bar = 2 µm

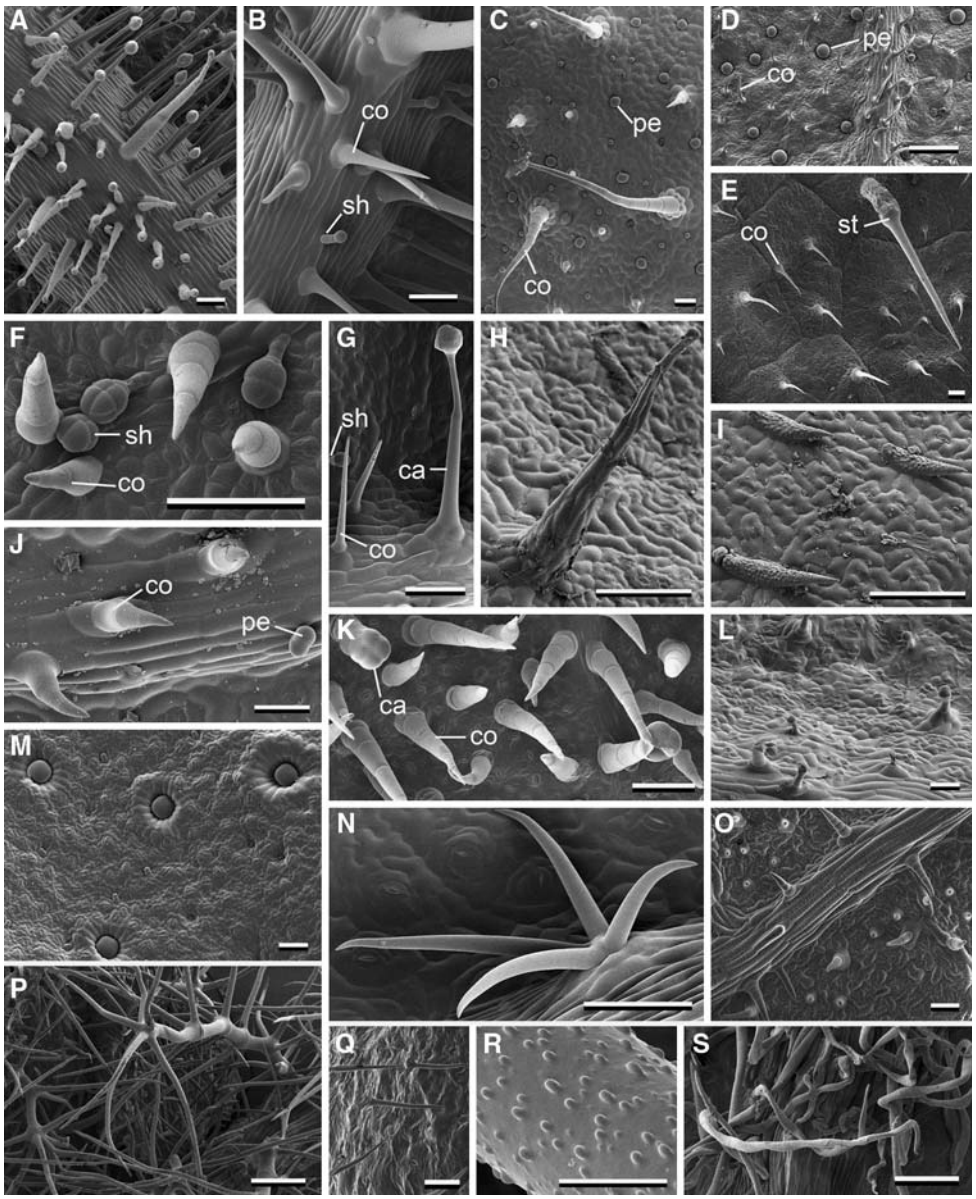

Fig. 6 Cryo-SEM micrographs of pubescent leaf surfaces used in the inversion test with *Dicyphus errans*. (**A**) *Datura innoxia*, abaxial side, capitate glandular trichomes. (**B**) *Borago officinalis*, abaxial side. (**C**) *Cissus njegerre*, adaxial side. (**D**) *Cissus njegerre*, abaxial side. (**E**) *Urtica dioica*, adaxial side. (**F**) *Lagenaria siceria*, adaxial side. (**G**) *Pelargonium zonale*, abaxial side. (**H**) *Cuphea lanceolata*, abaxial side, multiseriate trichome. (**I**) *Cuphea lanceolata*, adaxial side, spindle-shaped, procumbent, nodose trichomes. (**J**) *Ocimum basilicum*, adaxial side. (**K**) *Lagenaria siceria*, abaxial side. (**L**) *Calendula officinalis* 'Orangestrahlen', abaxial side, capitate trichomes. (**M**) *Ocimum basilicum*, abaxial side, peltate trichomes. (**N**) *Hibiscus rosa-chinensis*, abaxial side, star-shaped trichome. (**O**) *Tropaeolum majus*, abaxial side, cone-shaped trichomes and crystalline waxy coverage. (**P**) *Verbascum thapsus*, abaxial side, felt-like indumentum with tree-shaped trichomes. (**Q**) *Oenothera biennis*, adaxial side, cone-shaped trichomes. (**R**) *Oenothera biennis*, adaxial side, knobby surface, detail of a nodose trichome. (**S**) *Malus domestica*, abaxial side, thread-shaped and spiral-shaped, twisted trichomes. *co*, cone-shaped trichome; *sh*, stalked glandular head; *pe*, peltate trichome; *st*, stinging trichome; *ca*, capitate trichome. Scale bars: **A**–**Q**, **S** = 100 μm; **R** = 10 μm

Inversion experiment

Bug attachment to plant surface varied, depending on the plant species, surface type, leaf side, and insect sex (Fig. 8, Table 2). The attachment ability did not depend on the plant family. *D. errans* attached strongly (categories 2 and 3) to the adaxial leaf surfaces of 17 plant species, and to the abaxial leaf surfaces of 22 plant species. Generally, bugs attached better to pubescent plant substrates.

Significantly different attachment ability of bugs was shown for different plant surface types (Table 2). Surfaces covered with crystalline wax (*w*) strongly impeded

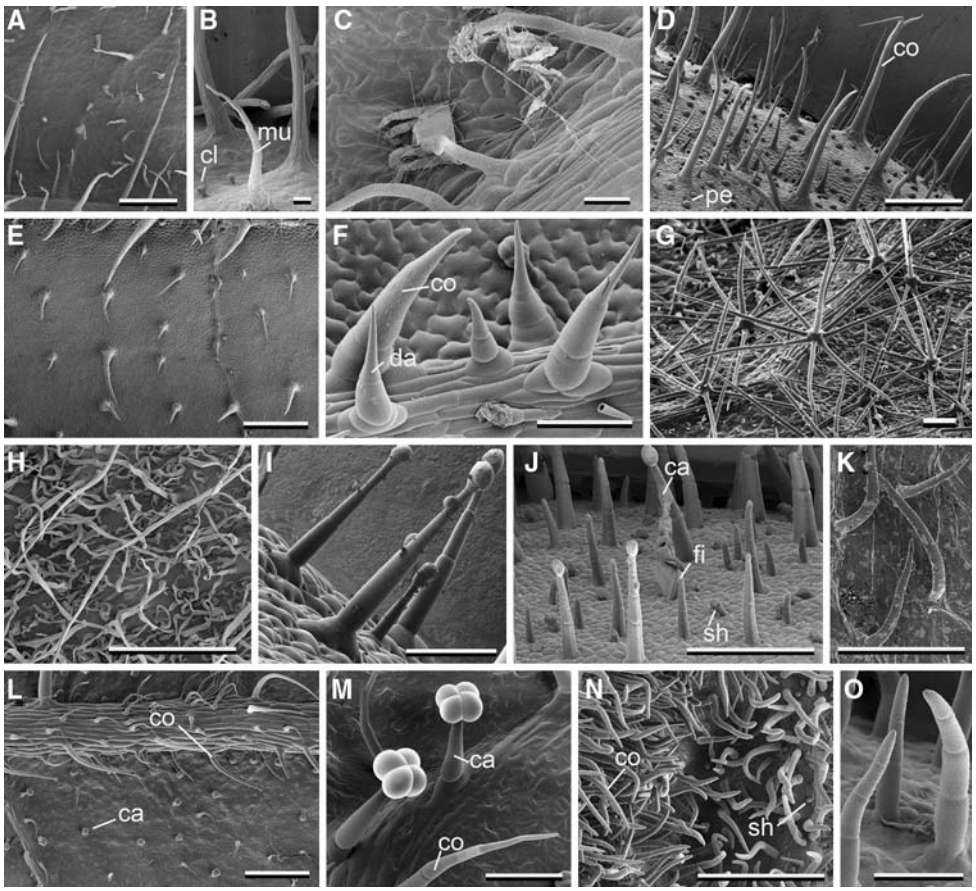

Fig. 7 Cryo-SEM micrographs of the abaxial leaf surfaces of pubescent plants used in the traction force test with *Dicyphus errans* females. (**A**) *Cleome hirsuticaulis.* (**B**) *Cleome hirsuticaulis*, multicellular and clavate trichomes in detail. (**C**) *Capsicum annuum* 'Yolo Wonder', finger-shaped trichomes. (**D**) *Plectranthus ambiguus.* (**E**) *Cucumis sativus* L. 'Rawa', cone-shaped trichomes marginally orientated. (**F**) *Cucumis sativus* 'Rawa'. (**G**) *Solanum melongena* L. 'Black Beauty', star-shaped trichomes. (**H**) *Gerbera jamesonii* × hybrida, felt-like indumentum. (**I**) *Petunia* × hybrida, capitate trichomes. (**J**) *Nicotiana sylvestris*. (**K**) *Fuchsia* × hybrida 'Winston Churchill', cone-shaped trichomes. (**L**) *Lycopersicon esculentum* 'Grit'. (**M**) *Lycopersicon esculentum*, capitate and cone-shaped trichomes. (**N**) *Digitalis purpurea* 'Excelsior'. (**O**) *Digitalis purpurea*, finger-shaped trichome in detail. *ca*, capitate; *cl*, clavate; *co*, cone-shaped; *da*, dart-shaped; *fi*, finger-shaped; *mu*, multi-cellular; *pe*, peltate; *sh*, stalked glandular head. Scale bars: **A**, **D**, **E**, **H**, **J**, **L**, **N** = 500 μm; **B**, **C**, **F**, **G**, **I**, **K**, **M**, **O** = 100 μm

attachment: in 91.7% of tests, the bug fell down immediately after inversion (category 0) or after inversion followed by light shaking (category 1). On surfaces with a combination of crystalline waxes and trichomes (*wh*), the attachment success was greater (e.g. *G. jamsonii* and the abaxial leaf side of *M. domestica*) than on waxy surfaces (*w*) without trichomes. As shown in Table 2, on the *wh* surface, categories 2 and 3 were significantly larger (category 2 + 3: 40%) than on the *w* surface (category 2 + 3: 8.3%) (χ^2 analysis of contingency tables, $\chi^2_{3,799} = 435.103$, $P \leq 0.001$). On the smooth surface (*s*) of *S. media*, bugs attached in 70% of the trials in category 2 and 30% in category 3. Except for the abaxial side of *C. annum* and *F.* × hybrida, as well as the adaxial side of *B. officinalis* and *O. basilicum*, inversions of the bug on surface types *hg*, *h*, and *g* resulted in the highest frequency of attachment in categories 2 and 3. On the majority of *hg* surfaces, bugs attached most frequently in category 2 (31.5%) and 3 (45.8%).

Females (61.3%) attached significantly better than males (58.0%) (χ^2 analysis of contingency tables, $\chi^2_{3,799} = 9.041$, $P \leq 0.029$).

The frequency of the optimum attachment (category 3) was significantly higher on the abaxial (41.5%) than on the adaxial (27.5%) leaf surfaces (χ^2 analysis of contingency tables, $\chi^2_{3,799} = 20.891$, $P \leq 0.001$).

Traction force experiment

The median force values varied considerably from 0.07 mN to 1.3 mN, depending on the plant substrate (Fig. 9). These values corresponded to between 1.8 and 34.2 times of the bug's body weight (3.8 ± 0.6 mg). The lowest force was measured on *B. oleracea* var. *gongylodes*, densely covered

Table 1 Trichome length, diameter, density per unit area, aspect ratio and measured adhesion force of 14 plant surfaces. Different letters in the right column indicate statistically significant differences between values (Kruskal–Wallis one way ANOVA on ranks, $H_{13,259} = 143.989$, $P \leq 0.001$ and Tukey test, $P < 0.05$)

No.	Plant species, cultivar	Trichome characteristics				Adhesion force [μN] median, signific., min.-max.
		Length [μm] mean ± sd (n)[1]	Diameter [μm] mean ± sd (n)[1]	Density [mm^{-2}] mean ± sd (n)[2]	Aspect ratio	
1	*Brassica oleracea var. gongylodes* 'Gigant'	–	–	–	–	6.6 [ad] (3.1–61.1)
2	*Capsicum annuum* 'Yolo Wonder'	262.1 ± 311.3 (38)	43.2 ± 3.7 (12)	70.6 ± 0.6 (5)	6.1	36.7 [bcde] (7.0–131.0)
3	*Cleome hirsuticaulis*	643.7 ± 254.3 (57)	87.7 ± 130.2 (18)	4.2 ± 1.7 (5)	7.3	83.4 [bc] (4.9–303.0)
4	*Cucumis sativus* 'Rawa'	439.5 ± 196.4 (150)	38.2 ± 13.3 (42)	7.0 ± 0.7 (5)	11.5	85.8 [bc] (4.4–192.0)
5	*Cyclamen persicum* 'Sierra F1'	–	–	–	–	4.7 [a] (1.9–321.0)
6	*Digitalis purpurea* 'Excelsior'	416.0 ± 143.4 (470)	40.4 ± 38.0 (15)	58.0 ± 2.6 (5)	10.3	16.2 [ac] (4.3–44.8)
7	*Fuchsia* x hybrida 'Winston Churchill'	348.1 ± 373.0 (60)	15.4 ± 7.7 (7)	2.6 ± 0.6 (5)	22.6	10.0 [ac] (0.9–317.0)
8	*Gerbera jamesonii* × hybrida	415.6 ± 260.3 (16)	25.8 ± 24.5 (27)	12.0 ± 0.8 (5)	16.1	4.5 [a] (2.8–205.0)
9	*Ibicella lutea*	399.7 ± 233.7 (36)	37.9 ± 14.0 (24)	17.4 ± 3.9 (5)	10.5	41.0 [bcd] (6.4–401.0)
10	*Lycopersicon esculentum* 'Grit'	550.6 ± 880.3 (328)	74.6 ± 30.4 (22)	40.2 ± 8.2 (5)	7.4	36.4 [bcd] (6.3–183.0)
11	*Nicotiana sylvestris*	323.8 ± 100.3 (100)	36.9 ± 9.5 (50)	25.6 ± 4.0 (5)	8.8	207.0 [b] (107.0–510.0)
12	*Petunia* × hybrida	355.3 ± 155.7 (218)	44.3 ± 13.5 (10)	13.1 ± 6.4 (5)	8.0	137.0 [b] (28.3–289.0)
13	*Plectranthus ambiguus*	650.4 ± 311.7 (338)	81.3 ± 98.9 (105)	8.1 ± 1.4 (5)	8.0	5.6 [ae] (1.4–47.7)
14	*Solanum melongena* 'Black Beauty'	468.0 ± 164.5 (175)	39.5 ± 7.7 (24)	3.8 ± 1.4 (5)	11,8	48.1 [bc] (26.4–165.0)

1) n, sample size of trichomes measured

2) n, sample size of areas with counted trichomes

with wax crystals, whereas the highest force was observed on *D. purpurea* having a mixed hairy and glandular hairy surface, and on the hairy surface of *S. melongena*.

Bugs performed better on pubescent surfaces than on waxy ones. Their force was significantly stronger on *L. esculentum*, *D. purpurea*, *P. ambiguus*, and *S. melongena* (Kruskal–Wallis one way ANOVA on ranks, $F_{14,149} = 105.095$, $P \leq 0.001$). The highest traction force was generated on *hg* substrates, followed by *wh*, *g*, and *h*. There was no significant difference between plants covered with trichomes and no correlation was found between measured force and the plant family. Qualitative properties of trichomes (shape, orientation, alignment etc.) did not influence the traction force, however, leaves covered with felt-like trichomes in *G. jamesonii* and *S. melongena* strongly enhanced the bugs' traction.

Considering the trichome morphometrical data, there was a significant correlation between the absolute traction force and (1) the length and (2) the diameter of trichomes (Fig. 10A, B) (linear regression, one way ANOVA). However, there was no correlation between the force and both trichome density and aspect ratio (Fig. 10C, D).

The comparision of traction experiment results and adhesive properties of pubescent (*h*, *hg*, and *g*) plants (see section "Plant surface characterisation") did not show any influence of plant adhesion on bug traction force (linear regression and one way ANOVA, Fig. 11A). However, if we consider only plant species from the *g* and *hg* surface types, a significantly negative correlation between the traction force and plant adhesion force became apparant (linear regression and one way ANOVA, Fig. 11B).

As shown in Table 3, the comparision of the traction force measured on the glass surface before and after testing on the plant substrate did not show pretarsus failure. In some cases, the force values on the glass were enhanced after the plant surface test (*C. hirsuticaulis*, *F.* × hybrida, *I. lutea*, *S. melongena*), although no clear trend could be recognized. A significant decrease of the traction force from 0.12 to 0.09 mN after walking on the leaf was observed only on the waxy *B. oleracea* (paired *t*-test, $T_{4,14} = 4.517$, $P = 0.011$). Bug median traction force on the glass surface before testing on the plant surface was 0.23 mN (6.1 times of body weight). SEM-micrographs demonstrate the degree of pretarsi contamination after walking on a plant surface (Fig. 12, Table 3). It ranged widely from 0 to 90% of the entire pretarsus area. The largest contaminated areas were found after walking on leaves of *B. oleracea* covered with wax crystals (60–90%). After walking on pubescent plant surfaces (*h*, *g*, *hg*) the contamination degree ranged between 0 and 80%.

Discussion

The attachment system of *Dicyphus errans*

Morphological and behavioural differences in gripping smooth and pubescent plant surfaces have been previously

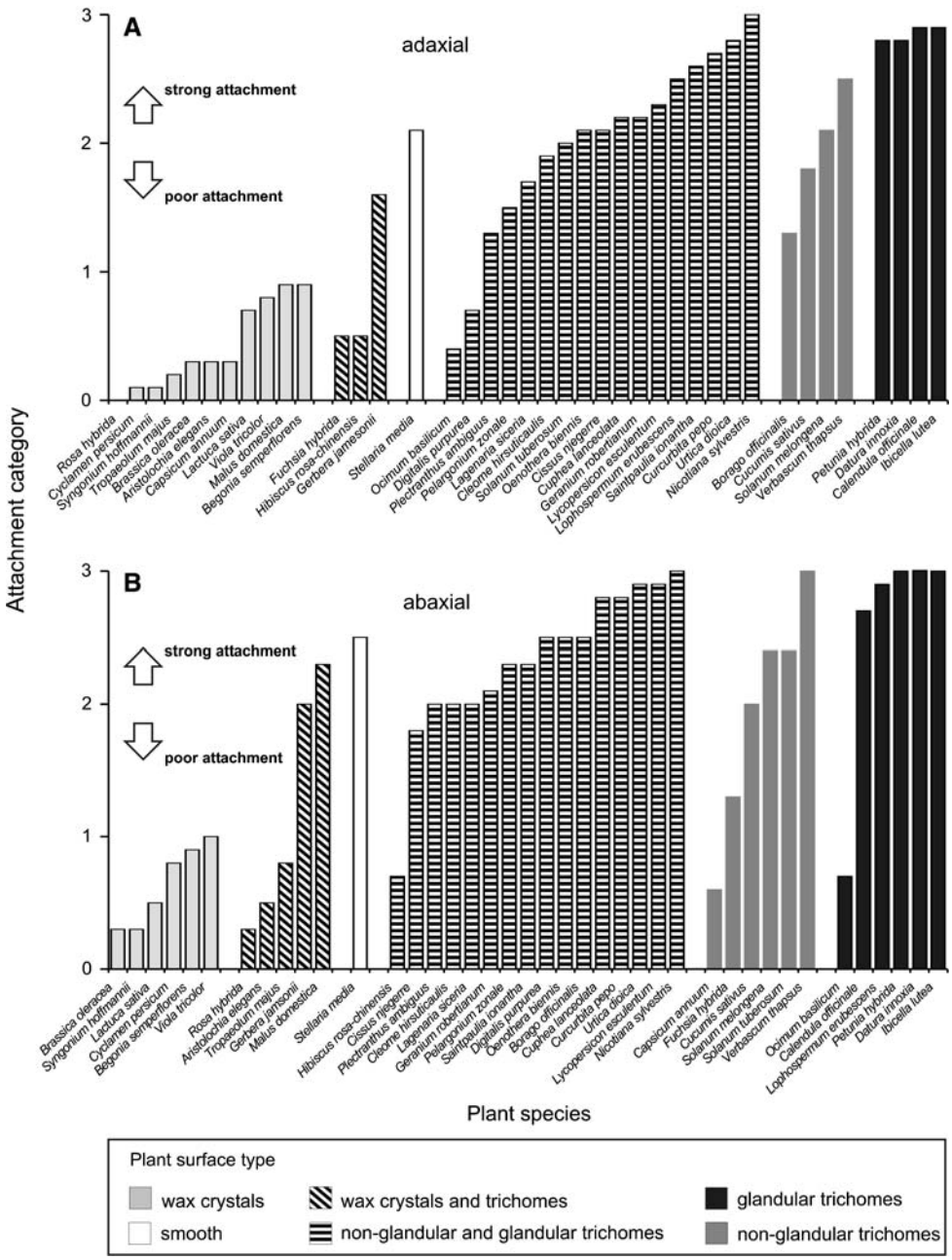

Fig. 8 Attachment ability of *Dicyphus errans* imagines in inversion tests with 40 plant species belonging to 25 plant families and 6 plant surface types; (**A**) Adaxial leaf side. (**B**) Abaxial side. (0) fell immediately after inverting, (1) fell after inverting and slight shaking (f = 2 Hz, A = 50 mm), (2) fell after inverting and strong shaking (f = 4 Hz, A = 100 mm), and (3) did not fall at all. (Mean scores, sample size: N = 10 adult *D. errans*, n = 5 repetitions per leaf surface)

shown in mirid bugs (Wheeler 2001). There are two basic strategies for adhereing to surfaces. On the one hand, curved elongated claws may interlock with rough substrates and plant trichomes. On the other hand, flexible pseudopulvilli enable mirid bugs to also attach to smooth surfaces (Wigglesworth 1959; Schuh 1976; Jordan 1962). *D. errans* bears an attachment system of the smooth type according to Gorb and Beutel (2001) and Gorb (2001). Structures found on the dorsal side of pseudopulvilli in *D. errans* (Fig. 3C) were previously reported for true bugs to be used to transport an adhesive secretion to the smooth ventral side of pulvilli (Ghazi-Bayat 1979; Ghazi-Bayat and Hasenfuß 1980, 1981). The secretion is essential in adhesion enhancement (Schuh and Slater 1995). While attaching to smooth surfaces, the claws are held at a very small angle to the ventral side of the legs and the paired claws forced apart. Thus, the ventral side of pseudopulvilli can come into contact with a substrate and peel off using the claws as a kind of lever. The therefore required flexibility of these structures is indicated by the presence of resilin in pseudopulvilli and in the membranous cuticle surrounding the unguitractor plate (Fig. 3A, B). Resilin has been previously reported in the tarsi of cockroaches (Frazier et al. 1999), ants (Federle et al. 2001), flies (Niederegger and Gorb 2003), wasps (Frantsevich and Gorb 2004), and several other insect species (Gorb 1996).

Table 2 Relative [%] and absolute (in parenthesis) frequencies of attachment ability categories of *Dicyphus errans* obtained in the inversion tests for various plant surface types, sex, and leaf side, as well as statistical differences between compared groups (χ^2 Analysis of Contingency Tables)

Compared groups	Frequencies of categories of attachment ability				Statistics
	0	1	2	3	
Plant surface types					
smooth (*s*)	0.0 (0)	0.0 (0)	70.0 (14)	30.0 (6)	$\chi^2_{3,799} = 435.103$, $P \leq 0.001$
waxy (*w*)	60.0 (108)	31.7 (57)	8.3 (15)	0.0 (0)	
waxy + hairy (*wh*)	32.9 (23)	27.1 (19)	30.0 (35)	10.0 (13)	
hairy + glandular hairy (*hg*)	7.9 (26)	14.8 (49)	31.5 (104)	45.8 (151)	
hairy (h)	8.9 (8)	24.4 (22)	40.0 (36)	26.7 (24)	
glandular hairy (*hg*)	4.5 (5)	5.5 (6)	10.0 (11)	80.0 (88)	
Sex					
female	18.0 (72)	20.8 (83)	23.3 (93)	38.0 (152)	$\chi^2_{3,799} = 9.041$, $P = 0.029$
male	24.5 (98)	17.5 (70)	27.0 (108)	31.0 (124)	
Leaf surface					
adaxial	26.0 (104)	20.5 (82)	26.0 (104)	27.5 (110)	$\chi^2_{3,799} = 20.891$, $P \leq 0.001$
abaxial	16.5 (66)	17.8 (71)	24.3 (97)	41.5 (166)	

(0) fell immediately after inversion, (1) fell after inversion and light shaking (f = 2 Hz, A = 50 mm), (2) fell after inversion and strong shaking (f = 4 Hz, A = 100 mm), and (3) did not fall at all

The elastic structural protein, resilin, is suggested to be responsible for the storage of elastic energy in joints, tendons, wings and other parts of the insect body (Anderson and Weis-Fogh 1964).

While adhering to a trichome, one part of the paired claws obviously interlocks with the middle region of the trichome, using the border of the basal claw plate and the ventro-distal claw surface. Four hypothesis of mirid bug interlocking mechanism on trichomes are proposed: (1) hooking the chiseled-sharpened ventro-distal claw surface and claw tooth to the trichome, (2) clinging to the trichome using the ventro-proximal surface and margins of the basal lobe-like thickening of the claw, (3) gripping the trichome using the ventral claw surface and pseudopulvillus (Southwood 1986), (4) surrounding the trichome with the claw concavity without using either the claw tooth or sharpened claw regions. An extremely small pretarsus makes live observations very difficult. Our experiment with Cryo-SEM showed that the assumed original interlocking site can be seen in the micrographs as a small horizontal groove (claw print) on the side wall of the capitate trichome (Fig. 3F), because the trichome and/or claw were slightly dislocated during the freezing and vacuum procedures. The "clawprint" groove indicates that sharpened claws grasp the flexible trichome surface to get a grip on the smooth wall, leaving an imprint. In contrast to a previous report (Southwood 1986), the use of pseudopulvilli by *D. errans* as an interlocking mechanism with trichomes could not be observed.

It could be conjectured that there should be an optimum range of trichome diameter for interlocking with curved claws. But morphometrical variables of the pretarsus do not indicate obvious specialisation of claw curvature to particular trichome geometry. It seems that claws are able to attach to a wide spectrum of plant trichomes. The diameter, measured in the middle of trichomes (39.5 μm) in the plant with the highest traction force (*S. melongena*, see Fig. 9) does not correspond to the diameter of a circle fitting the concavity of the claw (16.6 μm). We suggest three mechanisms explaining this. (1) Probably, the diameter of only the middle of trichomes is not crucial for mirid bug claw interlocking, but rather the mean diameter of the entire trichome. (2) A bug's claw may move up and down along the trichome until it finds the optimum diameter. (3) The already mentioned flexibility of the claw enables the bug to grip a range of trichomes having different diameters.

Bug attachment abilities

In the inversion experiment, forces acting on the insect were applied in a normal direction to the surface. *D. errans* was attached to the underside of a glass surface and tried to detach from it. Attachment of *D. errans* on substrates covered with wax crystals was poor. This result confirms previously reported observations for some Anthocoridae (Lauenstein 1976), Chrysomelidae (*Phaedon cochleariae* Fab., Stork 1980b, *C. fastuosa*, Gorb and Gorb 2002),

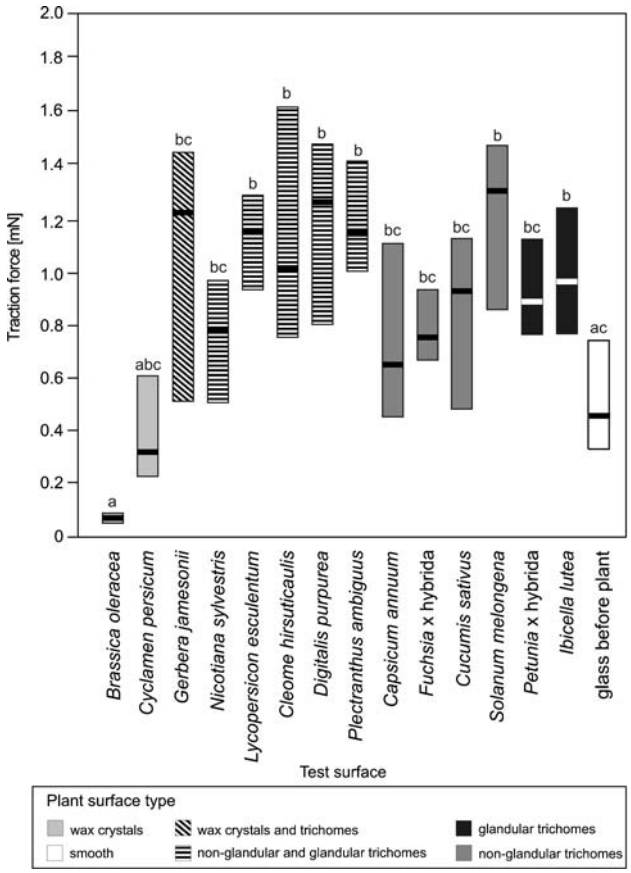

Fig. 9 Traction force generated by *Dicyphus errans* females on different plant species and surface types (median values are indicated by bold crossline). Different letters show significant differences between traction force values on different plant and glass surfaces (Kruskal–Wallis one way ANOVA on Ranks, $H_{14,149} = 105.095$, $P \leq 0.01$ and Dunn's method, $P < 0.05$)

Formicidae (*Oecophylla smaragdina* Fab., Federle et al. 2000), as well as several predatory insect species (Eigenbrode 2004). Gorb and Gorb (2002) proposed four hypotheses to explain reduced insect attachment on plant surfaces covered with crystalline epicuticular wax. These facts might explain some differences in attachment ability of bugs on different waxy surfaces in our inversion experiment.

On a smooth leaf surface of *S. media*, *D. errans* could attach properly. This may be explained by (1) small leaves where claws could cling to the leaf margin and (2) the ability of the mirid bug to attach to smooth surfaces using pseudopulvilli.

However, the results of the inversion experiment confirm strong adaptation of *D. errans* to a life on pubescent plants. The best attachment was found on hairy and even glandular hairy surfaces, e.g. *Lycopersicon esculentum*, where many other insects are not able to walk (e.g. Kennedy 2003). For example, the leaf beetle *Chrysolina fastuosa* L. (Chrysomelidae) was not able to attach to the upper surface of the leaf of this plant in inversion experiments (Gorb and Gorb 2002). Beetle tarsi, covered with adhesive hairs, glued together and were effectively disabled by the secretion of glandular trichomes.

General significantly stronger attachment of *D. errans* was found on abaxial leaf sides, than has been observed in inversion experiments with *C. fastuosa* (Gorb and Gorb 2002). These surfaces are usually rougher than adaxial ones. For *Rumex obtusifolius* L. (Polygonaceae), Hosoda and Gorb (2004) quantitatively demonstrated lower surface roughness on the adaxial leaf side. According to our data, abaxial surfaces bear trichomes more frequently and denser than adaxial ones. Intense coverage with trichomes correlates with the stronger bug attachment.

Inversion experiments with *C. fastuosa* (Gorb and Gorb 2002) and with *D. errans* in this study do not show that size and density of trichomes have a significantly quantitative effect on attachment. However, this test is not sophisticated enough to reveal differences between diverse surfaces covered with trichomes. Subsequent traction force tests demonstrated a higher resolution for quantifying substrate influence on bug attachment and locomotion.

In the traction force experiment, forces acting on the insect were applied in a lateral direction to the surface. *D. errans* generated force walking and pulling horizontally. Traction force corresponds to the friction between pretarsi of the insect and the substrate. High traction force, measured on hairy plant surfaces, confirms the results of our inversion experiment as well as previous assumptions by Southwood (1986) and Voigt (2005) that *D. errans* is adapted to, and has a close association with pubescent plant species. Considering trichome morphometry data, the trichome length and width seem to be the most essential variables, explaining measured forces (Fig. 10A, B). These variables effect claw interlocking. Longer and thicker trichomes are found to enhance bug traction force. We have not found any force dependence on trichome aspect ratio (Fig. 10D), although the aspect ratio should correlate with trichome bending stiffness and therefore influence the attachment strength of tarsi in contact. Trichome density has no significant influence on the attachment of *D. errans* (Fig. 10C) in contrast to some other entomophagous and phytophagous insect species, which are negatively affected by dense pubescence (Levin 1973; Fordyce and Agrawal 2001; Valverde et al. 2001). The ability of *D. errans* to attach on a wide range of pubescent plant surfaces with different trichome density may be a possible explanation of this effect.

Surfaces covered with glandular trichomes are the most adhesive ones. During locomotion, a bug must overcome the adhesion of the plant itself. We suppose that in contrast to less adhesive plant surfaces, on highly adhesive or rather sticky ones, bugs would move more carefully and therefore

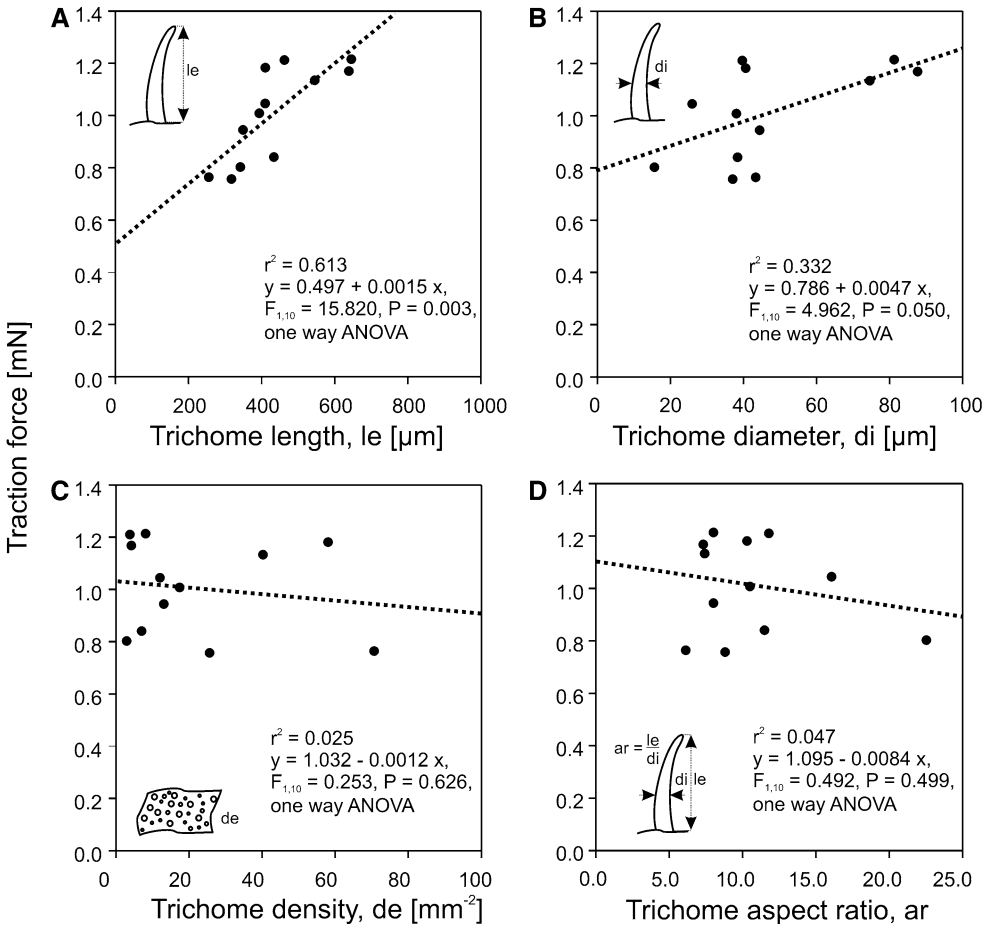

Fig. 10 Traction force versus morphometrical variables of trichomes. Mean force values versus the averaged trichome length (**A**), diameter (**B**), density (**C**), and aspect ratio (**D**). Dotted lines indicate linear regressions

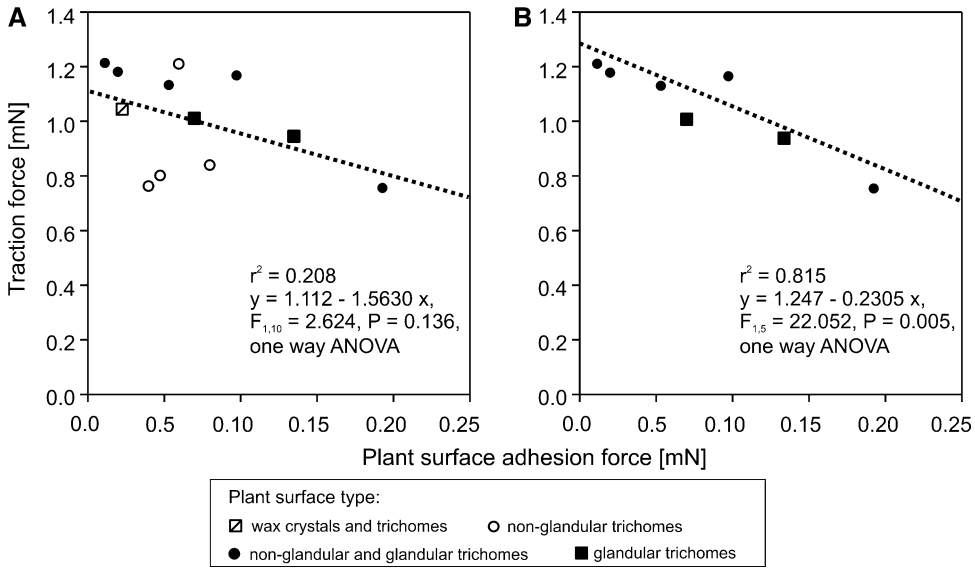

Fig. 11 Mean bug traction force versus mean plant surface adhesion force. (**A**) Data pooled together for all 12 pubescent plant species used. (**B**) Data for plant species with glandular trichomes or with a mixture of non-glandular and glandular trichomes only. Dotted lines indicate linear regressions

less powerfully. For this reason we measured plant surface adhesion and estimated its influence on the bug's traction force (Fig. 11). If we consider all 12 pubescent plant species studied, no relationship between plant adhesive properties and generated traction force was found (Fig. 11A). However, a significant negative correlation was found, if only *g* and *hg* surfaces are considered (Fig. 11B). Thus, we suggest that adhesive properties of the substrates, which are fully or partly covered with glandular trichomes, are remarkable influencing factors for bugs' traction force.

Table 3 Pretarsus contamination (in % of the entire pretarsus area) and measured traction force on glass surface before and after the walking on plant surface in the traction force experiment with *Dicyphus errans*

No.	Plant species, cultivar	Pretarsus contamination [% of the pretarsus area]	Traction force [mN]		
			On glass before on plant surface mean ± sd	On glass after on plant surface mean ± sd	Statistical differences between forces on glass (before vs. after)
1	*Brassica oleracea* var. *gongylodes* 'Gigant'	60–90	0.12 ± 0.05	0.09 ± 0.04	$T = 4.517$, $P = 0.011$
2	*Capsicum annuum* 'Yolo Wonder'	0–50	0.46 ± 0.15	0.43 ± 0.15	$T = 0.536$, $P = 0.620$
3	*Cleome hirsuticaulis*	0–50	0.19 ± 0.09	0.20 ± 0.09	$T = 1.262$, $P = 0.276$
4	*Cucumis sativus* 'Rawa'	0–80	0.14 ± 0.06	0.13 ± 0.10	$W = 5.000$, $P = 0.625$
5	*Cyclamen persicum* 'Sierra F1'	0–50	0.25 ± 0.10	0.17 ± 0.03	$T = 2.026$, $P = 0.113$
6	*Digitalis purpurea* 'Excelsior'	0–50	0.26 ± 0.08	0.13 ± 0.04	$T = 0.098$, $P = 0.927$
7	*Fuchsia* × hybrida 'Winston Churchill'	0–50	0.28 ± 0.17	0.35 ± 0.11	$T = 1.934$, $P = 0.125$
8	*Gerbera jamesonii* × hybrida	0–80	0.29 ± 0.08	0.26 ± 0.09	$T = 1.385$, $P = 0.238$
9	*Ibicella lutea*	0–80	0.21 ± 0.14	0.31 ± 0.33	$W = 7.000$, $P = 0.438$
10	*Lycopersicon esculentum* 'Grit'	50–80	0.34 ± 0.13	0.31 ± 0.23	$T = 0.469$, $P = 0.664$
11	*Nicotiana sylvestris*	0–80	0.23 ± 0.12	0.22 ± 0.08	$T = 0.421$, $P = 0.695$
12	*Petunia* × hybrida	0–50	0.17 ± 0.08	0.13 ± 0.04	$T = 1.338$, $P = 0.252$
13	*Plectranthus ambiguus*	50–80	0.29 ± 0.07	0.22 ± 0.08	$T = 2.480$, $P = 0.068$
14	*Solanum melongena* 'Black Beauty'	0–50	0.35 ± 0.15	0.36 ± 0.15	$W = 5.000$, $P = 0.625$

Statistics in the right column; *T*, paired *t*-test; *W*, Wilcoxon signed rank test; *P* = probability value

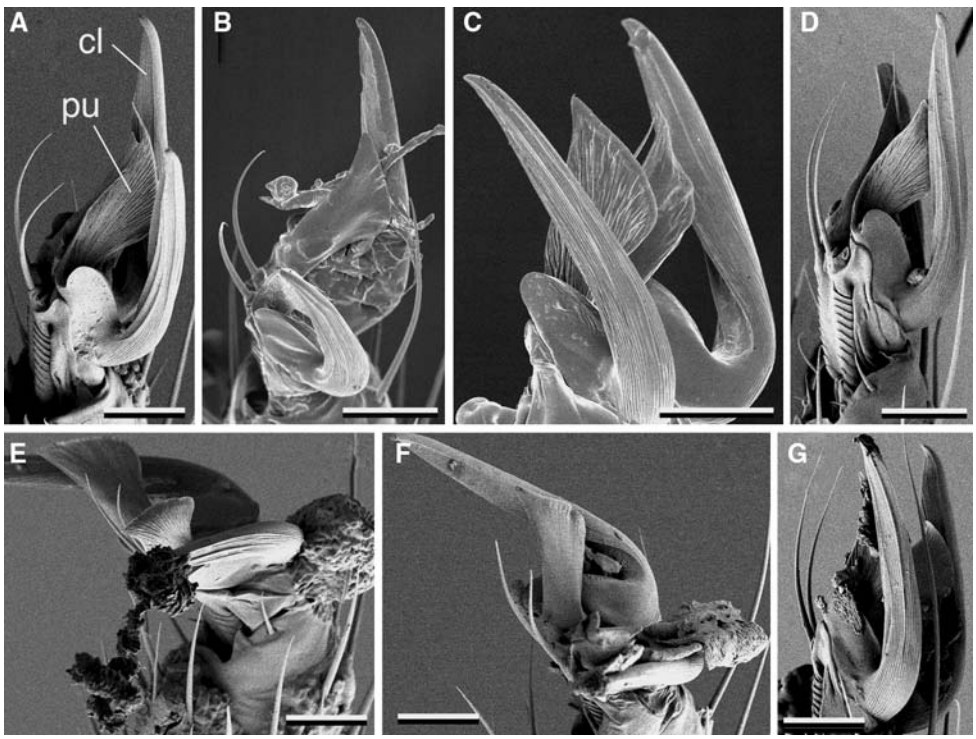

Fig. 12 SEM-micrographs of pretarsi of *Dicyphus errans* females after walking on different plant surfaces. (**A**) *Solanum melongena*, almost no claw contamination. (**B**, **C**) *Ibicella lutea*, heavy (**B**) and light (**C**) contamination. (**D**) *Cucumis sativus*, light contamination. (**E**) *Cleome hirsuticaulis*, heavy contamination. (**F**) *Lycopersicon esculentum*, heavy contamination. (**G**) *Plectranthus ambiguus*, heavy contamination. *cl*, claw; *pu*, pseudopulvilli. Scale bar = 25 µm

In contrast to this finding previous observations show that under field conditions, *D. errans* prefers to live on adhesive glandular plants (Voigt 2005). These plants provide many small arthropods, trapped by glandular trichomes, as prey for the bug and protect the latter from natural enemies, which are unable to walk on such surfaces (Voigt 2005). There may be a trade-off between higher energy effort and risk of walking on glandular plant surfaces, and the access to freshly captured prey at minimal competition and danger of predators.

Contamination of feet (Fig. 12) by slipping on glandular trichomes during traction could also be a reason for less

traction force generation on strongly adhesive surfaces. However, no considerable impact on the function of the attachment system walking on glass was found after walking on pubescent and glandular plant surfaces. *D. errans* possesses special cuticular protuberances and corresponding grooming behaviour for very extensive body grooming. These adaptations lead to the reduction of contamination and allow a life on pubescent and even glandular plant surfaces (Voigt 2005; Voigt et al. 2006). During the traction force experiment, insects were observed grooming themselves between individual tests. The generated traction force on glass (6.6 times of the bug body weight) indicates that attachment performance and ability to move in the bug is also rather strong on smooth surfaces, corresponding to the strong attachment on smooth plant substrate (*S. media*) in our inversion experiment.

The traction force on glass before and after walking on a plant surface significantly differed only in *Brassica oleracea*, which is densely covered with filamentous wax crystals (Table 3). SEM-micrographs showed contamination of 60–90% of the total tarsus area with wax crystals, which may support the contamination-hypothesis (Gorb and Gorb 2002). Foot contamination by wax crystals has previously been reported, in particular, for the beetles *P. cochleariae* (Stork 1980b), *Adalia bipunctata* L. (Gorb et al. 2005), and *C. fastuosa* (Gorb and Gorb 2006b).

Conclusions

Plant surfaces are important attachment substrates for phytophagous insects and their natural enemies. The omnivorous mirid bug *D. errans* inhabits pubescent, particularly glandular plant surfaces, which are avoided by many other entomophagous arthropods. The attachment ability of *D. errans* depends significantly on the plant surface type. Epicuticular crystalline waxes reduce bug attachment, whereas non-glandular and glandular trichomes, as well as the combination of both, promote attachment. Not only the presence of trichomes, but also their geometrical variables length and diameter influence attachment ability. The adhesion force of surfaces covered with glandular trichomes, as well as with a combination of non-glandular and glandular trichomes, has a negative correlation with the mirid bug's traction force. Direct mechanical contact between bug pretarsi and trichomes was visualized. We found that trichomes may provide suitable interlocking sites for attachment and locomotion of small specialised predatory insects, such as *D. errans*. Continued investigations on the anatomy and material properties of trichomes and bug pretarsi as well as eco-morphological studies will aid in further understanding of mechanical interactions between the bug and different types of plant surfaces.

Acknowledgements The first author thanks C. Neinhuis and the staff of the Botanical Garden as well as V. Pohris, M. Müller, and the staff of the Chair for Forest Protection at the Institute of Silviculture and Forest Protection, Faculty of Forestry, Geo and Hydro Sciences, Department of Forestry, Dresden University of Technology (Dresden, Germany) for providing space for the rearing of test plants and insects and for valuable discussions. The bug species were determined by K. Arnold (Geyer, Germany). The German companies Ernst Benary Samenzucht GmbH (Hann/Muenden), Quedlinburger Saatgut GmbH (Quedlinburg), Bruno Nebelung GmbH & Co. (Everswinkel), Cyclamen-Sprünken (Straelen), Eich Jungpflanzen Vertriebs GmbH (Grolsheim), Florensis Deutschland GmbH and Selecta Klemm GmbH & Co. KG (Stuttgart) provided seeds and seedlings. V. Kastner (Max-Planck Institute of Developmental Biology, Tübingen, Germany) helped with the experiments and linguistic corrections of the manuscript, and J. Schuppert (Max-Planck Institute for Metals Research, Stuttgart, Germany) with Cryo-SEM techniques. M. Varenberg (Max-Planck Institute for Metals Research, Stuttgart, Germany) and P. Perez Goodwyn (Graduated School of Agriculture, Kyoto University, Japan) are acknowledged for motivating discussion. The Federal Ministry of Education and Research, Germany (project BIOKON Phase II, 01RS0411) and the German National Academic Foundation (doctoral scholarship, E2002D0730) provided funding for the project.

Appendix

Below we provide a detailed description of the plant surfaces tested, according to the structural types shown in Fig. 4. Names of plant species are arranged alphabetically for quick access.

Aristolochia elegans Mart. (Aristolochiaceae) is covered with transversely ridged wax crystal rodlets, very densely distributed, almost without gaps, on the abaxial leaf side. There, sparsely distributed, inclined unicellular, hook-shaped trichomes are also found (Fig. 5A).

Begonia × *semperflorens* Link & Otto (Begoniaceae) has a smooth and shiny leaf surface. On the adaxial side, membraneous whole wax platelets are sparsely arranged (Fig. 5C). On the abaxial side, dispersed polygonal wax granules were found (Fig. 5B).

Borago officinalis L. (Boraginaceae) bears a densely hirsute indumentum, consisting of perpendicular and inclined, unicellular, tapered, cone-shaped, and strongly nodose trichomes on both leaf sides (Fig. 6B). Longer trichomes have a convex multicellular base, while shorter ones possess a convex unicellular base. Moreover, dispersed short capitate trichomes (stalked glandular heads) were found (Fig. 6B, see Fig. 4B, *S4*).

Brassica oleracea L. *var. gongylodes* L. 'Gigant' (Brassicaceae): the pruinouse surface of this plant is densely covered with filamentous wax crystals (polygonal rodlets and threads) (Fig. 5D).

Calendula officinale L. 'Orangestrahlen' (Compositae) has different trichomes on both leaf sides: (1) uniseriate, 2- to 10-celled and multiseriate, multicellular capitate trichomes with glandular heads (Fig. 6L), (2) rounded, cone-shaped, multicellular, glandular trichomes without a head, and (3) sparsely dispersed capitate trichomes (stalked glandular heads, see Fig. 4B, *S4*).

Capsicum annuum L. 'Yolo Wonder' (Solanaceae) has a smooth appearing adaxial leaf surface that bears very sparsely dispersed wax crystals, arranged in groups from 3 to 10 platelets (Fig. 5I). Groups of numerous curved, finger-shaped, unicellular trichomes occur in the leaf domatia on the abaxial leaf surface (Fig. 7C).

Cissus njegerre Gilg (Vitaceae), a tropical liana, has a pilose indumentum. On the adaxial leaf side, following trichomes occur: (1) regularly dispersed, bent, uniseriate, 5- to 11-celled ones, (2) perpendicular, 2- to 3-cellular, cone-shaped, nodose trichomes with multicellular convex base, and (3) several dispersed, 1- and 4-celled, peltate trichomes (Fig. 6C). The abaxial leaf surface is covered with regularly dispersed, strongly curved, cone-shaped, uniseriate, 2-celled trichomes with one convex basal cell, as well as with bent, 5- to 11-cellular, nodose trichomes with a multi-cellular convex base, mostly with distally oriented tips (Fig. 6D). The trichomes are more densely concentrated along leaf veins. Moreover, perpendicular 2- to 4-cellular capitate trichomes are scattered all over the leaf lamina. The abaxial leaf surface is also covered with 1- and 4-cellular peltate trichomes.

Cleome hirsuticaulis J. F. Macbr. (Capparidaceae): the leaves have a pilose indumentum, which is most dense along leaf veins and on the abaxial side (Fig. 7A). It consists of dispersed, both inclined and bent, multiseriate, multicellular, cone-shaped glandular trichomes with small glandular heads and a multicellular convex base. Very long and slightly shorter trichomes of this type were found. Multicellular clavate trichomes as well as uniseriate, 3- to 10-cellular trichomes (Fig. 7B) seldom occur.

Cucumis sativus L. 'Rawa' (Curcurbitaceae): the hirsute indumentum shows regularly dispersed, perpendicular (or inclined), uniseriate, uni- to 4-cellular, tapered cone-shaped (or dart-shaped) trichomes with a multi-cellular base (Fig. 7E, F). The trichome density is higher on the adaxial leaf side. Trichomes are orientated towards the leaf margin.

Cuphea lanceolata W. T. Aiton (Lythraceae): regularly dispersed, unicellular, spindle-shaped, nodose trichomes were found on the leaf. They are procumbent and located close to the leaf surface (Fig. 6I). Only the trichome tip and the distal half are bent away from the lamina at an angle of approximately 45°. On the abaxial side, trichomes occur more densely along leaf veins and sparsely in the intercostal areas. Besides, long inclined, multiseriate, multicellular trichomes with small glandular heads are scattered on both leaf sides (Fig. 6H).

Curcurbita pepo L. 'Hokkaido' (Curcurbitaceae) possesses a dense (adaxial side), and sparse (abaxial side) hirsute pubescence, consisting of regularly dispersed, perpendicular and inclined, uniseriate, 3- to rarely 5-cellular, tapered cone-shaped trichomes with thickened bases, as well as sparse 2-celluar capitate trichomes. Trichomes are most densely concentrated along leaf veins.

Cyclamen persicum Mill. 'Sierra F1' (Primulaceae) the leaves bear, on the adaxial side, sparsely distributed, single, entire wax platelets. On the abaxial lamina surface, these can be also clustered in rosettes (Fig. 5K).

Datura innoxia Mill. (Solanaceae) shows a pilose indumentum, composed of dispersed, uniseriate, 3- to 5-cellular, inclined, cone-shaped, nodose and capitate trichomes (Fig. 6A). The adaxial pubescence is denser than the abaxial one.

Digitalis purpurea L. 'Excelsior' (Scrophulariaceae) has dispersed, bent, uniseriate, 3- to 5-cellular, nodose, cone-shaped, partially finger-shaped trichomes, distributed very densely along leaf veins (Fig. 7N, O). Sparsely dispersed, inclined capitate trichomes (stalked 2-cellular glandular heads, Fig. 7N) and capitate ones with 4-cellular heads were also found.

Fuchsia × hybrida Hort. ex Vilm 'Winston Churchill' (Onagraceae): the adaxial leaf side possesses sparsely dispersed, inclined (on veins also bent), unicellular, thread-like and spiral-shaped, nodose trichomes with a rounded tip and a convex unicellular base. The surface is also covered with individual, entire, crystal wax platelets, often arranged in clusters (Fig. 5H). On the abaxial side, trichomes are inclined, bent and curved, unicellular, cone- and spiral-shaped, and nodose with a convex unicellular base, concentrated along the leaf vein and sparsely dispersed in the intercostal areas (Fig. 7K).

Geranium robertianum L. (Geraniaceae) bears bent, 2- to 4-cellular, capitate, nodose trichomes with a multicellular base as well as sparse, inclined, unicellular, cone-shaped, nodose trichomes on the abaxial leaf side. Capitate trichomes (stalked glandular heads, see Fig. 4B, *S4*) cover the entire surface. On the abaxial leaf side, dense, curved, unicellular, thread-shaped trichomes as well as inclined 4-cellular, capitate, nodose trichomes were found on the leaf veins. Additionally, stiff cone-shaped, nodose trichomes with a multicellular base and capitate trichomes (stalked glandular heads) are present.

Gerbera jamesonii × hybrida Adlam (Compositae): the adaxial leaf side is covered with sparse, inclined and bent uniseriate 4-cellular thread-shaped trichomes as well as dispersed clusters of membranous crystalline wax platelets. The felt-like indumentum of the abaxial surface along and around the leaf veins consists of inclined, bent, curved, uniseriate, multi-cellular, spiral-shaped, often twisted trichomes with convex unicellular bases (Fig. 7H). Inclined,

bent, curved, uniseriate, multicellular, spiral-shaped trichomes as well as occasional, entire crystal wax platelets also appear sparsely in the intercostal areas.

Hibiscus rosa-chinensis L. (Malvaceae) shows the following surface structures on the adaxial leaf surface: (1) inclined and bent, unicellular trichomes on leaf veins, (2) sparsely distributed, 4-cellular peltate trichomes in the intercostal areas as well as wax crystals (clusters of membraneous and entire platelets) (Fig. 5F). On the abaxial side, there are inclined and bent, unicellular trichomes, and 2- to 8-cellular stellate trichomes on the leaf veins (Fig. 6N) as well as sparsely distributed 4-cellular peltate trichomes in the intercostal areas.

Ibicella lutea (Lindl.) Van Eselt. (Martynaceae) is densely covered with the following trichomes: (1) glandular-pubescent, perpendicular and inclined, uniseriate, 3- to 8-cellular, capitate with convex unicellular base, (2) perpendicular, uniseriate, 4-cellular, cone-shaped, (3) perpendicular, 3-cellular, finger-shaped, (4) multicellular clavate, and (5) peltate.

Lactuca sativa L. 'Attraktion' (Asteraceae): membraneous wax platelets, arranged as rosettes, are found on the adaxial leaf surface (Fig. 5E). On the abaxial surface there are clusters of irregular wax platelets.

Lagenaria siceria (Mol) Stadley (Curcurbitaceae) exhibits a pilose coverage, consisting of (1) capitate trichomes with an unicellular stem and 4-cellular head, (2) perpendicular and inclined, uniseriate 2- to 5-cellular, dart-shaped, nodose trichomes with thickened basal cell, (3) dispersed 4-cellular peltate trichomes as well as (4) stalked 4-cellular heads (Fig. 6K). Trichomes are located sparsely on the adaxial side and densely on the abaxial surface, and concentrated especially along leaf veins.

Lophospermum erubescens D. Don (Scrophulariaceae): the leaf surface is covered with dispersed perpendicular, 3- to 4-celled, cone-shaped glandular trichomes of different length, with glandular head or with rounded tip, and always with one convex basal cell. Clavate trichomes are regularly dispersed.

Lycopersicon esculentum Mill. 'Grit' (Solanaceae) bears regularly dispersed (1) 2-cellular, bent and curved, tapered, cone-shaped, nodose trichomes with convex unicellular bases, (2) inclined and bent, uniseriate, 3- to 5-cellular, cone-shaped, nodose glandular trichomes, (3) sporadic uniseriate, 5- to 12-cellular, cone-shaped trichomes with a multi-cellular base, and (4) capitate trichomes with 4-cellular glandular heads; these are mainly concentrated along leaf veins (Fig. 7L, M).

Malus domestica Borkh. (Rosaceae): the leaf surface appears adaxially smooth with sparsely occurring irregular, membraneous wax platelets arranged in clusters (Fig. 5M), whereas on the abaxial side, a felt-like pubescence was found (Fig. 6S). The inclined and bent unicellular thread-shaped and spiral-shaped, partly twisted trichomes are concentrated along the leaf veins. Besides, sparsely occurring irregular wax crystal platelets arranged in clusters are present on both the trichomes and lamina surface (Fig. 5L).

Nicotiana sylvestris Spegazz. et Gomez (Solanaceae) is covered with (1) dispersed inclined, 2- to 6-cellular, capitate, (2) cone-shaped, glandular trichomes, (3) stalked glandular heads, (4) perpendicular, 2- to 5-cellular finger-shaped trichomes with a convex unicellular base. They all were concentrated along the leaf veins (Fig. 7J).

Ocimum basilicum L. (Lamiaceae): the surface is smooth with some dispersed 1-, 2- and 4-cellular peltate trichomes (Fig. 6M). Cone-shaped, nodose, tapered trichomes are present along the adaxial veins (Fig. 6J).

Oenothera biennis L. (Onagraceae): regularly dispersed, inclined and bent, unicellular, cone-shaped, nodose, tapered trichomes as well as clavate ones were found on the adaxial leaf side (Fig. 6Q, R). The abaxial, felt-like indumentum consists of (1) curved thread-shaped trichomes, (2) dispersed, inclined and bent unicellular cone-shaped tapered nodose trichomes, and (3) densely distributed clavate trichomes.

Pelargonium zonale (L.) L'Hérit. (Geraniaceae): the adaxial lamina side is predominantly covered with regularly dispersed, inclined and bent, unicellular, cone-shaped, tapered trichomes with a slightly thickened base. Inclined, 2- to 4-cellular capitate trichomes with uni- and multicellular bases as well as regularly dispersed, capitate trichomes (stalked glandular heads, Fig. 4B, *S4*) were also found. The abaxial leaf surface bears mainly (1) regularly dispersed, inclined 2- to 4-cellular capitate trichomes with a uni- and multicellular base, but also (2) regularly dispersed capitate trichomes (stalked glandular heads, see Fig. 4B, *S4*) as well as (3) irregularly dispersed, inclined and bent, unicellular, cone-shaped, tapered trichomes with slightly thickened bases (Fig. 6G).

Petunia × hybrida Vilm. (Solanaceae): the pilose, glandular indumentum consists of dispersed perpendicular and inclined uniseriate 1- to 3-, rarely 5-cellular capitate trichomes (Fig. 7I).

Plectranthus ambiguus (Bolus) Codd. (Lamiaceae) has a pilose indumentum on both leaf sides with (1) regularly dispersed, inclined and bent, on the veins especially curved, uniseriate, 4- to 15-cellular, cone-shaped, tapered, nodose trichomes with convex multicellular base, (2) dispersed 4-cellular peltate trichomes, (3) capitate trichomes (stalked glandular heads, see Fig. 4B, *S4*), and (4) sparsely occurring perpendicular 2- to 4-cellular capitate trichomes (Fig. 7D).

Rosa × hybrida L. 'Bernstein' (Rosaceae) bears adaxially, sparsely dispersed, irregular wax crystal platelets arranged in small groups (Fig. 5J). On the abaxial leaf side, very sparsely dispersed, irregular wax platelets, and unicellular peltate trichomes are present.

Saintpaulia ionantha Wendl. (Gesneriaceae) possesses a pilose indumentum, consisting of (1) densely dispersed,

inclined, bent and curved, uniseriate, 2- to 12-cellular, cone-shaped, tapered trichomes, rarely with small rounded glandular heads, and (2) 1- to 4-cellular peltate trichomes.

Solanum melongena L. 'Black Beauty' (Solanaceae): the felt-like hairy coverage exhibits multicellular, stellate nodose trichomes, consisting of 5–9 branches, with the central branch perpendicularly oriented and other branches, arising perpendicularly from the central one, in a ray-like manner around it (Fig. 7G). Trichomes are very densely distributed along veins and on the abaxial side. Inclined, unicellular, cone-shaped trichomes were found only on the adaxial leaf surface.

Solanum tuberosum L. 'Acapella' (Solanaceae) is covered with regularly dispersed, inclined, uniseriate, 3- to 5-cellular, nodose trichomes as well as clavate ones, which are denser on the abaxial side than on the adaxial one.

Stellaria media (L.) Vill. (Caryophyllaceae): the leaf lamina is smooth without any crystalline waxes or trichomes. Cell irregularities determine the surface topography.

Syngonium auritum Schott (Araceae): leaves appear shiny with membraneous and irregular wax platelets, arranged in rosettes. Crystals on the abaxial side are much more densely distributed around the stomata (Fig. 5N).

Tropaeolum majus L. (Tropaeolaceae) is densely covered with tubular wax crystals on the glaucous adaxial leaf surface. The abaxial side bears scattered, perpendicular, and inclined, uniseriate, 2- to 6-cellular, cone-shaped trichomes with a convex unicellular base. The entire surface here, including the trichomes, is densely covered with tubular wax crystals (Fig. 5G, 6O).

Urtica dioica L. (Urticaceae) has (1) inclined, unicellular, cone-shaped, nodose trichomes, (2) stinging trichomes, and (3) bent, unicellular, cone-shaped, nodose trichomes with thickened bases. Trichomes are orientated distally.

Verbascum thapsus L. (Scrophulariaceae): the felt-like indumentum consists abaxially of bent multicellular branched, tree-shaped (dendroid) trichomes (Fig. 6P). Additionally, 4- to 6-cellular stellate trichomes are located on the adaxial side of the leaf.

Viola tricolor L. (Violaceae) has a smooth appearing surface with polygonal wax crystal plates arranged in groups, partially covering the stomata on the abaxial leaf side (Fig. 5O).

References

Andersen SO, Weis-Fogh T (1964) Resilin, a rubber-like protein in arthropod cuticle. Adv Insect Physiol 2:1–65

Andow DA, Prokrym DR (1990) Plant structural complexity and host-finding by a parasitoid. Oecologia 82:62–165

Andres MR, Connor EF (2003) The community-wide and guild-specific effects of pubescence on the folivorous insects of manzanitas *Arctostaphylos* spp. Ecol Entomol 28:383–396

Arzet H-R (1972) Suchverhalten und Nahrungsverbrauch der Larven von *Chrysopa carnea* Steph. Dissertation, Georg-August-Universität, Göttingen, Germany, pp. 93

Avé DA, Gregory P, Tingey WM (1987) Aphid repellent sesquiterpenes in glandular trichomes of *Solanum berthaultii* and *S. tuberosum*. Entomol Exp Appl 44:131–138

Barthlott W, Neinhuis C, Cutler D, Ditsch F, Meusel I, Theisen I, Wilhelmi H (1998) Classification and terminology of plant epicuticular waxes. Botan J Linn Soc126:237–260

Becerra JX (2003) Synchronous coadaption in an ancient case of herbivory. PNAS 100:12804–12807

Begon M, Townsend CR, Harper JL (2006) Ecology: from individuals to ecosystems, 4th edn. Blackwell Publishing Ltd., 738 pp

Belcher DW, Thurston R (1982) Inhibition of movement of larvae of the convergent lady beetle by leaf trichomes of tobacco. Environ Entomol 11:91–94

Benedict HJ, Leigh TF, Hyer AH (1983) *Lygus hesperus* (Heteroptera: Miridae) oviposition behaviour, growth, and survival in relationship to cotton trichome density. Environ Entomol 12:331–335

Bernays EA, Chapman RF (1994) Host-plant selection by phytophagous insects. Contemporary topics in entomology, 2nd edn. Chapman & Hall, pp. 312

Betz O (2002) Performance and adaptive value of tarsal morphology in rove beetles of the genus *Stenus* (Coleoptera, Staphylinidae). J Exp Biol 205:1097–1113

Brennan EB, Weinbaum SA (2001) Stylet penetration and survival of three psyllid species on adult leaves and 'waxy' and 'de-waxy' juvenile leaves of *Eucalyptus globulus*. Entomol Exp Appl 100:355–363

Carter MC, Sutherland D, Dixon AFG (1984) Plant structure and the searching efficiency of coccinellid larvae. Oecologia 63:394–397

Chapman RF (1977) The role of leaf surface in food selection by acridids and other insects. Coll Int CNRS 265:133–149

Coll M, Smith LA, Ridgway RL (1997) Effect of plants on the searching efficiency of a generalist predator: the importance of predator-prey spatial associations. Entomol Exp Appl 83:1–10

Coll M (1998) Living and feeding on plants in predatory heteroptera. In: Coll M, Ruberson JR (eds) Predatory Heteroptera: their ecology and use in biological control. Proc Entomol Soc Am, pp 89–130

Cortesero AM, Stapel JO, Lewis WJ (2000) Understanding manipulating plant attributes to enhance biological control. Biol Control 17:35–49

Dalin P, Björkman C, Eklund K (2004) Leaf beetle grazing does not induce willow trichome defence in the coppicing willow *Salix viminalis*. Agr Forest Entomol 6:105–109

Dixon AFG (1986) Habitat specifity and foraging behaviour of aphidophagous insects. In: Hodek I (ed) Ecology of aphidophaga. Proceedings of the 2nd symosium held at Zvíkovské Podhradí, September 2–8, 1984, Series Entomologica 35, pp 151–154

Dos Santos TM, Júnior ALB, Soares JJ (2003) Influência de tricomas do algodoeiro sobre os aspectos biológicos e capacidade predatória de *Chrysoperla externa* (Hagen) alimentada com *Aphis gossypii* Glover. Bragantia, Campinas 62:243–254

Duffey SS (1986) Plant glandular trichomes: their partial role in defense against insects. In: Juniper B, Southwood R (ed) Insects and the plant surface. Edward Arnold Publishers, London, pp 151–172

Ecole CC, Picanço MC, Guedes RNC, Brommonschenkel SH (2001) Effect of cropping season and possible compounds involved in the resistance of *Lycopersicon hirsutum* f. *typicum* to *Tuta absoluta* (Meyrick) (Lep., Gelechiidae). J Appl Entomol 125:193–200

Eigenbrode SD (1996) Plant surface waxes and insect behaviour. In: Kerstiens G (eds) Plant cuticles—an integral functional approach. BIOS Publ., Oxford, pp 201–222

Eigenbrode SD (2004) The effects of plant epicuticular waxy blooms on attachment and effectiveness of predatory insects. Arthr Struct Dev 33:91–102

Eigenbrode SD, Castagnola T, Roux M-B, Steljes L (1996) Mobility of three generalist predators is greater on cabbage with glossy leaf wax than on cabbage with a wax bloom. Entomol Exp Appl 81:335–343

Eisner T, Eisner M, Hoebeke ER (1998) When defense backfires: detrimental effect of a plant's protective trichomes on an insect beneficial to the plant. Proc Natl Acad Sci USA 95:4410–4414

Elsey KD (1974) Influence of plant host on searching speed of two predators. Entomophaga 19:3–6

Esau K (1965) Plant anatomy, 2nd edn. John Wiley & Sons, pp 767

Evans HF (1976) Mutual interference between predatory anthocorids. Ecol Entomol 1:283–286

Federle W, Brainerd WL, McMahon T, Hölldobler B (2001) Biomechanics of the movable pretarsal adhesive organ in ants and bees. PNAS 98:6215–6220

Federle W, Maschwitz U, Fiala B, Riederer M, Hölldobler B (1997) Slippery ant-plants and skilful climbers: selection and protection of specific ant partners by epicuticular wax blooms in *Macaranga* (Euphorbiaceae). Oecologia 112:217–224

Federle W, Rohrseitz K, Hölldobler B (2000) Attachment forces of ants measured with a centrifuge: better "wax-runners" have poorer attachment to a smooth surface. J Exp Biol 203:505–512

Fordyce JA, Agrawal AA (2001) The role of plant trichomes and caterpillar group size on growth and defence of the pipevine swallowtail *Battus philenor*. J Anim Ecol 70:997–1005

Frantsevich L, Gorb S (2004) Structure and mechanics of the tarsal chain in the hornet, *Vespa crabro* (Hymenoptera: Vespidae): implications on the attachment mechanism. Arthr Struct Dev 33:77–89

Frazier SF, Larsen GS, Neff D, Quimby L, Carney M, DiCaprio RA, Zill SN (1999) Elasticity and movements of the cockroach tarsus in walking. J Comp Physiol A 185:157–172

Gassmann AJ, Hare JD (2005) Indirect cost of a defensive trait: variation in trichomes type affects the natural enemies of herbivorous insects on *Datura wrightii*. Oecologia 144:62–71

Gaume L, Perret P, Gorb E, Gorb S, Labat J-J, Rowe N (2004) How do plant waxes cause flies to slide? Experimental tests of wax-based trapping mechanisms in three pitfall carnivorous plants. Arthr Struct Dev 33:103–111

Gepp J (1977) Bewegungsbehinderung von Arthropoden durch Trichome an Bohnenpflanzen (*Phaseolus vulgaris* L.). Anz Schädlingskde Pflanzenschutz Umweltschutz 50:8–12

Ghazi-Bayat A (1979) Zur Oberflächenstruktur der tarsalen Haftlappen von *Coreus marginatus* (L.) (Coreidae, Heteroptera). Zool Anz 203:345–347

Ghazi-Bayat A, Hasenfuss I (1980) Die Oberflächenstrukturen des Prätarsus von *Elasmucha ferrugata* (Fabricius) (Acanthosomatidae, Heteroptera). Zool Anz 205:76–80

Ghazi-Bayat A, Hasenfuss I (1981) Über den Transportweg der Haftflüssigkeit der Pulvilli bei *Coptosoma scutellatum* (Geoffr.) (Plataspididae, Heteroptera). Nachrichtenblatt der Bayerischen Entomologen 30:58

Gibson RW (1971) Glandular hairs providing resistance to aphids in certain wild potato species. Ann Appl Biol 68:113–119

Gibson RW, Pickett JA (1983) Wild potato repels aphids by release of aphid alarm pheromone. Nature 302:608–609

Gilbert LE (1971) Butterfly-plant coevolution: has *Passiflora adenopoda* won the selectional race with Heliconiine butterflies? Science 172:585–586

Gingras D, Boivin G (2002) Effect of plant structure, host density and foraging duration on host finding by *Trichogramma evanescens* (Hymenoptera: Trichogrammatidae). Environ Entomol 31:1153–1157

Goffreda JC, Mutschler MA, Avé DA, Tingey WM, Steffens JC (1989) Aphid deterrence by glucose esters in glandular trichome exudate of the wild tomato, *Lycopersicon pennelli*. J Chem Ecol 15:2135–2147

Gorb E, Gorb S (2006a) Combination of the surface profile and chemistry reduces the attachment of the beetle *Gastrophysa viridula* on the *Rumex obtusifolius* leaf surface. Proceedings of the 5th plant biomechanics conference, August 28th–September 1st, 2006, vol 2. Stockholm, Sweden, pp 537–542

Gorb E, Gorb S (2006b) Do plant waxes make insect attachment structures dirty? Experimental evidence for the contamination hypotheses. In: Herrel A, Speck T, Rowe NP (eds) Ecology and biomechanics. CRC Press, Taylor & Francis, Boca Raton, Florida, pp 147–162

Gorb EV, Gorb SN (2002) Attachment ability of the beetle *Chrysolina fastuosa* on various plant surfaces. Entomol Exp Appl 105:13–28

Gorb E, Haas K, Henrich A, Enders S, Barbakadze N, Gorb S (2005) Composite structure of the crystalline wax layer of the slippery zone in the pitchers of the carnivorous plant *Nepenthes alata* and its effect on insect attachment. J Exp Biol 208:4651–4662

Gorb E, Kastner V, Peressadko A, Arzt E, Gaume L, Rowe N, Gorb S (2004) Structure and properties of the glandular surface in the digestive zone of the pitcher in the carnivorous plant *Nepenthes ventrata* and its role in insect trapping and retention. J Exp Biol 207:2974–2963

Gorb SN (1996) Design of insect unguitractor apparatus. J Morphology 230:219–230

Gorb SN (1999) Serial elastic elements in the damselfly wing: mobile vein joints contain resilin. Naturwissenschaften 86:552–555

Gorb SN (2001) Attachment devices of insect cuticle. Kluwer Academic Publishers, Dordrecht, pp 305

Gorb SN, Beutel RG (2001) Evolution of locomotory attachment pads of hexapods. Naturwissenschaften 88:530–534

Goundoudaki S, Tsitsipis JA, Margaritopoulos JT, Zarpas KD, Divanidis S (2003) Performance of the tobacco aphid *Myzus persicae* (Hemiptera: Aphididae) on oriental and Virginia tobacco varieties. Agr Forest Entomol 5:285–291

Gregory P, Ave DA, Bouthyette PJ, Tingey WM (1986) Insect-defensive chemistry of potato glandular trichomes. In: Juniper B, Southwood R (eds) Insects and the plant surface. Edward Arnold Publishers, London, pp 173–184

Grevstad FS, Klepetka BW (1992) The influence of plant architecture on the foraging efficiencies of a suite of ladybird beetles feeding on aphids. Oecologia 92:399–404

Grimaldi D, Engel MS (2004) Evolution of the insects. Cambridge University Press, New York, pp 755

Haddad NM, Hicks WM (2000) Host pubescence and the behavior and performance of the butterfly *Papilio troilus* (Lepidoptera: Papilionidae). Environ Entomol 29:299–303

Hare JD (2005) Biological activity of acyl glucose esters from *Datura wrightii* glandular trichomes against three native insect herbivores. J Chem Ecol 31:1475–1491

Hare JD, Elle E (2002) Variable impact of diverse insect herbivores on dimorphic *Datura wrightii*. Ecology 83:2711–2720

Hare JD, Smith II JL (2005) Competition, herbivory, and reproduction of trichome phenotypes of *Datura wrightii*. Ecology 86:334–339

Hoffmann GD, McEvoy PB (1985) The mechanism of trichome resistance in *Anaphalis margaritacea* to the meadow spittlebug *Philaenus spumarius*. Entomol Exp Appl 39:123–129

Hosoda N, Gorb SN (2004) Critical roughness for insect attachment: experimental evidences for the beetle *Gastrophysa viridula*. Abstracts of 2 Bremer Bionik-Kongress, 29.-30.10.2004, Bremen

Hoxie RP, Wellso SG, Webster JA (1975) Cereal leaf beetle response to wheat trichome length and density. Environ Entomol 4:365–370

Hummel K, Staesche K (1962) Die Verbreitung der Haartypen in ihren natürlichen Verwandtschaftsgruppen. In: Zimmermann W, Ozenda PG (eds) Handbuch der Pflanzenanatomie, Gebrüder Bornträger, Berlin, 2. v. neub. Aufl., Band IV, Teil 5. Abteilung: Histologie, Gebrüder Borntraeger, Berlin-Nikolassee, pp 207–292

Jeffree CF (1986) The cuticle, epicuticular waxes and trichomes of plants, with reference to their structure, functions and evolution. In: Juniper B, Southwood R (eds) Insects and the plant surface. Edward Arnold Publishers, London, pp 23–64

Jervis M, Kidd N (1996) Insect natural enemies. Practical approaches to their study and evaluation. Chapman & Hall, London, 491 pp

Johnson B (1953) The injurious effects of the hooked epidermal hairs of french beans (*Phaseolus vulgaris* L.) on *Aphis craccivora* Koch. Bull Entomol Res 44:779–788

Johnson B (1956) The influence on aphids of the glandular hairs on tomato plants. Plant Pathology 5:131–132

Johnson HB (1975) Plant pubescence: an ecological perspective. Bot Rev 41:233–258

Jolivet P (1998) Interrelationship between insects and plants. CRC Press, Boca Raton, Florida, 309 pp

Jordan KHC (1962) Landwanzen. Die neue Brehm-Bücherei, Bd. 294, A.-Ziemsen-Verlag, Wittenberg-Lutherstadt, 116 pp

Juniper BE (1995) Waxes on plant surfaces and their interactions with insects. In: Hamilton RJ (ed) Waxes: chemistry, molecular biology and functions. Oily, West Ferry, Dundee, pp 157–174

Juniper BE, Jeffree CE (1983) Plant surfaces. Edward Arnold Limited, London, 93 pp

Kareiva P, Sahakian R (1990) Tritrophic effects of a simple architectural mutation in pea plants. Nature 345:433–434

Kashyap RK, Kennedy GG, Farrar RR Jr (1991) Behavioral response of *Trichogramma pretiosum* Riley and *Telenomus sphingis* (Ashmead) to trichome/methyl ketone mediated resistance in tomato. J Chem Ecol 17:543–556

Keller MA (1987) Influence of leaf surfaces on movements by the hymenopterous parasitoid *Trichogramma exiguum*. Entomol Exp Appl 43:55–59

Kennedy CEJ (1986) Attachment may be a basis for specialization in oak aphids. Ecol Entomol 11:291–300

Kennedy GG (2003) Tomato, pests, parasitoids, and predators: tritrophic interactions involving the genus *Lycopersicon*. Annu Rev Entomol 48:51–72

Kowalewski E, Robinson RW (1978) White fly species resistance in *Cucumis* species. Cucurbit Genetics Cooperative Report 1:38

Kullenberg B (1946) Studien über die Biologie der Capsiden. Zool Bidrag Uppsala 23:1–522

Lapointe SL, Tingey WM (1986) Glandular trichomes of *Solanum berthaultii* confer resistance to green peach aphid (Homoptera: Aphididae). J Econ Entomol 79:1264–1268

Lauenstein G (1976) Untersuchungen zu Biologie und Verhaltensweisen der Räuberischen Blumenwanze *Anthocoris nemorum* L. (Het.: Anthocoridae). Dissertation, G.-August-Universität Göttingen, Germany

Lee YI, Kogan M, Larsen JR Jr (1986) Attachment of the potato leafhopper to soybean plant surfaces as affected by morphology of the pretarsus. Entomol Exp Appl 42:101–107

Lees AD, Hardie J (1988) The organs of adhesion in the aphid *Megoura viciae*. J Exp Biol 136:209–228

Leite GLD, Picanço M, Della Lucia TMC, Moreira MD (1999) Role of canopy height in the resistance of *Lycopersicon hirsutum* f. *glabrum* to *Tuta absoluta* (Lep., Gelechiidae). J Appl Entomol 123:459–463

Levin DA (1973) The role of trichomes in plant defense. Quart Rev Biol 48:3–15

Malakar R, Tingey WM (2000) Glandular trichomes of *Solanum berthaultii* and its hybrids with potato deter oviposition and impair growth of potato tuber moth. Entomol Exp Appl 94:249–257

McKinney KB (1938) Physical characteristics on the foliage of beans and tomatoes that tend to control some small insect pests. J Econ Ent 31:630–631

Metcalfe CR, Chalk L (1988) Anatomy of the dicotyledons. Leaves, stem, and wood in relation to taxonomy with notes on economic uses, vol II, 2nd edn. Oxford University Press, 330 pp

Müller C (2006) Plant-insect interactions on cuticular surface. In: Riederer M, Müller C (eds) Biology of plant cuticle. Blackwell Publishing, Oxford, pp 398–422

Musetti L, Neal JJ (1997) Resistance to the pink potato aphid, *Macrosiphum euphorbiae*, in two accessions of *Lycopersicon hirsutum* f. *glabratum*. Entomol Exp Appl 84:137–146

Napp-Zinn K (1973) Anatomie des Blattes. II Blattanatomie der Angiospermen. A. Entwicklungsgeschichte und topographische Anatormie des Angiospermenblattes. In: Linsbauer K (ed) Handbuch der Pflanzenanatomie, Bd. VIII, Teil 2 A, Bornträger-Verlag, Berlin

Niederegger S, Gorb S (2003) Tarsal movements in flies during leg attachment and detachment on a smooth substrate. J Ins Physiol 49:611–620

Obrycki JJ (1986) The influence of foliar pubescence on entomophagous species. In: Boerthel DJ, Eikenbarry RD (eds) Interactions of plant resistance and parasitoids and predators of insects. J. Wiley & Sons, New York, 200 pp

Obrycki JJ, Tauber MJ (1984) Natural enemy activity on glandular pubescent potato plants in the greenhouse: An unreliable predictor of effects in the field. Environ Entomol 13:679–683

Payne WW (1978) A glossary of plant hair terminology. Brittonia 30:239–255

Peeters PJ (2002) Correlations between leaf structural traits and the densities of herbivorous insect guilds. Biol J Linnean Soc 77:43–65

Pillemer EA, Tingey WM (1978) Hooked trichomes and resistance of *Phaseolus vulgaris* to *Empoasca fabae* (Harris). Entomol Exp Appl 24:83–94

Putman WL (1955) Bionomics of *Stethorus punctillum* Weise (Coleoptera: Coccinellidae) in Ontario. Can Entomol 86:9–33

Quilici S, Iperti G (1986) The influence of host plant on the searching ability of first instar larvae of *Propylea quadrodecimpunctata*. In: Hodek I (ed) Ecology of aphidophaga. Series Entomologica 35:99–111

Rabb RL, Bradley JR (1968) The influence of host plants on parasitism of eggs of the tobacco hornworm. J Econ Entomol 61:1249–1252

Ranger CM, Hower AA (2002) Glandular trichomes on perennial alfalfa affect host-selection behavior of *Empoasca fabae*. Entomol Exp Appl 105:71–81

Ringlund K, Everson EH (1968) Leaf pubescence in common wheat, *Triticum aestivum* L., and resistance to the cereal leaf beetle, *Oulema melanopus* (L.). Crop Science 8:705–710

Roberts JJ, Foster JE (1983) Effect of leaf pubescence in wheat on the bird cherry oak aphid (Homoptera: Aphidae). J Econ Entomol 76:1320–1322

Rudgers JA, Strauss SY, Wendel JF (2004) Trade-offs among anti-herbivore resistance traits: insights from Gossypieae (Malvaceae). Am J Bot 91:871–880

Schoonhoven LM, van Loon JA, Dicke M (2005) Insect-plant biology, 2nd edn. Oxford University press, New York, 421 pp

Schuh RT (1976) Pretarsal structure in the Miridae (Hemiptera) with a cladistic analysis of relationships within the family. Am Mus Novit 2601:1–39

Schuh RT, Slater JA (1995) True bugs of the world (Hemiptera: Heteroptera): Classification and natural history. Cornell University Press, London, 336 pp

Seidenstücker G (1967) Eine Phyline mit *Dicyphus*-Kralle (Heteroptera, Miridae). Reichenbachia Bd. 8. 27:215–220

Sengonca C, Gerlach S (1984) Einfluss der Blattoberfläche auf die Wirksamkeit des räuberischen Thrips, *Scolothrips longicornis* (Thysan.: Thripidae). Entomophaga 29:55–61

Shanower TG, Romeis J, Peter AJ (1996) *Pigeonpea* plant trichomes: Multiple trophic level interactions. In: Ananthakrishnan TN (ed) Biotechnological perspectives in chemical ecology of insects. Oxford & IBH, New Delhi, pp 76–88

Shah MA (1980) Beutesuchverhalten von Coccinelliden. Dissertation, Universität Hohenheim, Germany

Shah MA (1982) The influence of plant surfaces on the searching behaviour of coccinellid larvae. Entomol Exp Appl 31:377–380

Simmons AT, Gurr GM (2004) Trichomes-based host plant resistance of *Lycopersicon* species and the biocontrol agent *Mallada signata*: are they compatible? Entomol Exp Appl 113:95–101

Simmons AT, Gurr GM (2005) Trichomes of *Lycopersicon* species and their hybrids: effects on pests and natural enemies. Agr Forest Entomol 7:265–276

Simmons AT, Gurr GM, McGrath D, Martin PM, Nicol HI (2004) Entrapment of *Helicoverpa armigera* (Hübner) (Lepidoptera: Noctuidae) on glandular trichomes of *Lycopersicon* species. Australian J Entomol 43:196–200

Simmons AT, Gurr GM, McGrath D, Nicol HI, Martin PM (2003) Trichomes of *Lycopersicon* spp. and their effect on *Myzus persicae* (Sulzer) (Hemiptera: Aphidiae). Australian J Entomol 42:373–378

Smith CM (2005) Plant resistance to arthropods. Springer, Dordrecht, 423 pp

Southwood TRE (1973) The insect/plant relationship—an evolutionary perspective. Symp Roy Entomol Soc London 6:3–30

Southwood R (1986) Plant surfaces and insects-an overview. In: Juniper B, Southwood R (ed) Insects and the plant surface. Edward Arnold Publishers, London, pp 1–22

Stork NE (1980b) Role of wax blooms in preventing attachment to brassicas by the mustard beetle, *Phaedon cochleariae*. Entomol Exp Appl 28:100–107

Stork NE (1986) The form of plant waxes: a means of preventing insect attachment? In: Juniper B, Southwood R (eds) Insects and the plant surface. Edward Arnold Publishers, London, pp 346–347

Thurston R (1970) Toxicity of trichome exudates of *Nicotiana* and *Petunia* species to tobacco hornworm larvae. J Econ Entomol 63:272–274

Thurston R, Webster JA (1962) Toxicity of *Nicotiana gossei* domin to *Myzus persicae* (Sulzer). Entomol Exp Appl 5:233–238

Thurston R, Smith WT, Cooper BP (1966) Alkaloid secretion by trichomes of *Nicotiana* species and resistance to aphids. Entomol Exp Appl 9:428–423

Uphof JCT (1962) Plant hairs. In: Zimmermann W, Ozenda PG (eds) Handbuch der Pflanzenanatomie, Gebrüder Bornträger, Berlin, 2. v. neub. Aufl., Band IV, Teil 5, Abteilung: Histologie, Gebrüder Borntraeger, Berlin-Nikolassee, pp 1–206

Valverde PL, Fornoni J, Núnez-Farfán J (2001) Defensive role of leaf trichomes in resistance to herbivorous insects in *Datura stramonium*. J Evol Biol 14:424–432

Van Dam NM, Hare JD (1998) Differences in distribution and performance of to sap-sucking herbivores on glandular and non-glandular *Datura wrightii*. Ecol Entomol 23:22–32

Voigt D (2004) Relevanz der Pflanzen im Räuber-Beute-(Wirts-) Pflanzen-Komplex der Weichwanze *Dicyphus errans* Wolff (Heteroptera, Miridae, Bryocorinae). Mitteilungen der BBA, Berlin-Dahlem 396:480

Voigt D (2005) Untersuchungen zur Morphologie, Biologie und Ökologie der räuberischen Weichwanze *Dicyphus errans* Wolff (Heteroptera, Miridae, Bryocorinae). Dissertation, TU Dresden, Germany, http://nbn-resolving.de/urn:nbn:de:swb:14-1138036391273-82564

Voigt D, Pohris V, Wyss U (2006) Zur Nahrungsaufnahme von *Dicyphus errans* Wolff (Heteroptera, Miridae, Bryocorinae): Nahrungsspektrum, Potenzial und Verhalten. Mitt Dtsch Ges Allg Angew Ent 15:305–308

Wagner E (1955) Bemerkungen zum System der Miridae (Hemiptera, Heteroptera). Dtsch Entomol Z 2:230–242

Walters PJ (1974) A method for culturing *Stethorus spp*. (Coleoptera: Coccinellidae) on *Tetranychus urticae* (Koch) (Acarina: Tetranychidae). J Aust Ent Soc 13:245–246

Wheeler AG (2001) Biology of the plant bugs (Hemiptera: Miridae): Pests, predators, opportunists. Cornell University Press, London, pp. 507

Wigglesworth VB (1959) Physiologie der Insekten. Reihe Exp. Biologie, Bd. 14, Birkhäuser Verlag, Basel & Stuttgart, 2. Aufl

Zvereva EL, Kozlov MV, Niemelä P (1998) Effects of leaf pubescence in *Salix borealis* on host-plant choice and feeding behaviour of the leaf beetle, *Melasoma lapponica*. Entomol Exp Appl 89:297–303

Zwölfer H (2003) Insekten und Pflanzen. In: Dettner K, Peters W (eds) Lehrbuch der Entomologie. Spektrum Akademischer Verlag, Heidelberg, 2. neub. Aufl, pp 499–520